Design of a Efficient Turbofan Engine with Afterburner(s)

A project presented to
The Faculty of the Department of Aerospace Engineering
San Jose State University

In partial fulfillment of the requirement for the degree
Master of Science in Aerospace Engineering

By

Justin M. Williams

December 2022

Approved by

Dr. Yawo Ezunkpe
Faculty Advisor

ABSTRACT

Design of a Efficient Turbofan Engine with Afterburner(s)

Justin M. Williams

The objective of this project was to study and improve the overall efficiency of the turbofan engine while incorporating an afterburner(s) into its engine cycle. A turbofan engine was chosen with its engine components broken down for investigation. The modelling and simulation of the turbofan engine that included afterburners was done using GasTurb and MATLAB software packages. There were different characteristics that was investigated such as the specific thrust, fuel-to-air mass ratio, thrust-specific fuel consumption, thermal efficiency, propulsive efficiency, and overall efficiency. The results from the characteristics were compared and visualized through plots using MATLAB code. These plots help to identify any recurring patterns that the turbofan engine with an afterburner would experience. In addition to that, GasTurb software was used to analyze the 3-D plots that allowed for a complete understanding of how the efficiency of the turbofan engine was affected. As a result, the performance values were discovered that measured the turbofan engine components such as the intake, fan, intermediate-pressure compressor, high-pressure compressor, burner, high-pressure turbine, intermediate-pressure turbine, low-pressure turbine and the nozzle. Lastly, it was discovered that a turbofan engine with an afterburner is an efficient engine.

Acknowledgements

I would like to first thank my Lord and Savior Jesus Christ for all that he has blessed me with. Second my I would like to thank my Mom and Brother for being there for me.

Table of Contents

List of Tables

List of Figures

Nomenclature

Symbol	Definition
A	A Nozzle Exit Area
a	Acceleration
A*	Nozzle Throat Area
$A_{total\ nozzle\ exit}$	Total surface area of the nozzle exit
AR	Area Ratio (AR)
AR*	Equivalent Area Ratio
atm	Atmosphere
CV	Control Volume
F	Force
k	Kelvin
M	Mass
m/s	Meters per second
M_dot	Mass flow rate
P_c	Chamber Pressure
$P_{exhaust}$	Exhaust flow Pressure
P_e	Pressure at nozzle exit
ρ	Density
ρ_c	Density in chamber
T	Temperature
V_{exit}	Velocity exit
M	Mach Number
t	Time
Re	Reynolds Number
S	Area
V_0, V_e	Velocities at inlet and exit
P_0, P_e	Pat inlet and exit
F_T	Uninstalled thrust
S_T	Uninstalled thrust specific fuel consumption
T_T	Installed engine thrust
TSFC	Installed thrust specific fuel consumption
$mdot_f$	Mass flow rate of fuel
n_T	Thermal efficiency of engine
$Wdot_{out}$	Netpower out of engine
$Qdot_{in}$	Rate of thermal energy released
N_T	Propulsive efficiency of engine
T_p	Thrust of propulsion system
V_0	Velocity of aircraft
$Wdot_{out}$	Net power out of engine
$P_0, T_0, M_0, c_p, T_r, \pi_r$	Flight Conditions
$(c_p T_t)_{burner\ exit}$	Design Limits

π_d, π_b, π_n	Components Performance
π_c, π_f	Design Choices

Chapter 1 – Introduction

1.1 Motivation

The majority of commercial aircrafts are designed by gas turbine engines, which are either turbofan or turboprop. When it comes to the design of a turbofan engine, many engineers are trying to increase the efficiency of the turbofan engine without effecting the fuel consumption, performance, endurance, etc. Most modern-day commercial airplanes use a turbo fan engine because of the high thrust it produces and also because of the good fuel efficiency that it has. Many turbofan engines consist of the air inlet/fan section, compressor section, combustion section, turbine section and the exhaust/nozzle section. Many modern-day designers are focusing more on the power generation of the engine. In turn, this brings to conversation on the efficiency and performance aspects of the turbofan engine while including an afterburner.

The development of the propulsion system for a turbofan engine has had a lot of complex challenges. Most of the challenges was because of its multidimensional systems. There are different propulsion systems with higher efficiency that would decrease the amount of fuel and hence the environmental impact, especially the release of CO_2 [1]. There are different theory's that prove that the turbofan engine is one of the most fuel-efficient airplane engines that has been developed. With the state-of-art technology that we have there are different ways that the overall efficiency of the turbofan engine can be improved. One way is to use the Adaptive Cycle Engine (ACE) concept. The Adaptive Cycle Engine (ACE) concept is proven to meet the demands of the turbofan engine in terms of performance requirements. The ACE has low specific fuel consumption in subsonic flight. The ACE model involves two different thermodynamic cycles (turbojet and turbofan) on the same system, which makes the aircraft replies multi-purpose missions both in supersonic and subsonic flight [2]. Furthermore, since the ACE model involves a changing by-pass ratio, it would be considered to have more advantages in regards to the overall efficiency, flight range and specific fuel consumption.

With all this in consideration, the main purpose of the present study is to study and improve the overall efficiency of the turbofan engine while incorporating an afterburner(s) into its engine cycle for commercial airplanes. The approach and procedures will follow the different sources included in this report that was used to analyze and design turbofan engines. A realistic design approach for the inclusion of afterburner(s) to a turbofan engine will be discussed throughout this report to provide more insight into the possibilities of this design.

1.2 Literature Review

Before the analysis was done for the current project a literature review was done involving how to improve the overall efficiency of a turbofan engine. This was done in order to get a better understanding of the concept.

Another literature review was done involving afterburner(s). This was also done to get a better understanding of the concept of an afterburner. Lastly, one final literature review was done

involving the overall efficiency of the turbofan engine while incorporating an afterburner(s) into its engine cycle. The following sections summarize each literature review finds and their contribution to the project.

1.2.1 Overall Efficiency of a Turbofan Engine Studies

1.2.1.1 Energy and Performance Optimization of an Adaptive Cycle Engine for Next Generation Combat Aircraft

This study looked at how the Adaptive Cycle Engine (ACE) was one of the top methods that would fulfill the many multi-mission requirements of aircraft flight. This concept dealt with the deficiencies of conventional low by-pass mixed turbofan engines. This study explained how two different methods are used to optimize the overall efficiency of a turbofan engine. The first method looked at the performance and design results of the ACE model and compared it with those of fixed cycle low by-pass turbofan engine by using specific fuel consumption, specific thrust, power and efficiency parameters [3]. The second method looked at the different ways the design parameters such as, the ST and SFC values of the ACE model are analyzed for double by-pass mode and single by-pass mode [4]. Overall, this study provides a well-developed approach to how to optimize the overall efficiency of a turbofan engine which can be referenced for this project.

1.2.1.2 Exergy Modeling for Evaluating Sustainability Level of a High By-Pass Turbofan Engine Used on Commercial Aircrafts

This study presents an exergy modeling to evaluate the sustainability level of a high by-pass turbofan engine used on commercial aircrafts [5]. The PW4056 model turbofan engine was used to examine its sustainability under different flight conditions. As a result, a sustainability analysis was done to improve the exergy efficiency of the engine. Furthermore, this study provides what is needed to know to optimize the overall efficiency of a turbofan engine for this report.

1.2.1.3 Parametric Study on Exergy and NOx Metrics of Turbofan Engine Under Different Design Variables

This study examined the different effects of design variables on performance parameters for turbofan engines. This study looked at the effects of the by-pass ratio and turbine inlet temperatures for a turbofan engine. The parametric cycle equations regarding turbofan engines are encoded so as to compute performance metrics, while conducting energy analysis. Overall, this study looked at ways to improve and to find out optimum design variables in terms of eco-friendly aircraft activities [6].

1.2.1.4 Exergy and Thermoeconomic Analysis of a Turbofan Engine During A Typical Commercial Flight

This article examined the design and improvement of energy conversion systems for a turbofan engine. The article presented an exergy-based analysis which analyzed the performance of a typical turbofan engine and its components. The analysis was meant to simulate the exergy efficiency over the entire flight cycle for commercial flight. From that the data gathered was used to model aircrafts for commercial flight. Overall, this article provides the exergy and thermoeconomic approaches in order to improve the efficiency of a turbofan engine.

1.2.1.5 An Exergy Way to Quantify Sustainability Metrics for A High Bypass Turbofan Engine

This study examined a new methodology to meet the need of the growing concern of fuel efficiency for the design and operation of the turbofan engine. The new methodology is being developed here that proposes the use of exergetic metrics for mapping the exergy flows throughout high bypass turbofan engine at maximum thrust level for its sustainability assessment [7]. The engine that was used for this study had a net thrust force of 206 kN and was used in the first wide body, dual-aisle, and the largest commercial aircraft [8]. The study found that the exergetic sustainability method was an effective way to assess the sustainability of aircraft and aero engines and provides a good tool for designers, users, decision makers and researchers in green air transportation [9]. Following the study, it was found that the method made turbofan engines more sustainable for flight. Furthermore, this article will serve as a good reference to help improve the overall efficiency of a turbofan engine.

1.2.1.6 Turbofan engine performances from aviation, thermodynamic and environmental perspectives

This study examined how the JT15D turbofan engine and its main subcomponents were assessed with the aviation, energy, exergy, environmental, and sustainability analyses [10]. These different subcomponents were analyzed in order to make the turbofan engine more efficient. After the analysis it was found that the combustion chamber has minimum rates of sustainable efficiency factor, exergetic efficiency and sustainability index, while it has utmost rates of ecological and environmental effect factors, fuel exergy waste ratio, irreversibility and productivity lack ratios [11]. Finally, it was found that the combustion chamber and the low-pressure compressor components should be optimized for better performance of the system. Overall, this study provides an approach to how to optimize the overall efficiency of a turbofan engine which can be referenced for this project.

1.2.1.7 Impact of different fuel usages on thermodynamic performances of a high bypass turbofan engine used in commercial aircraft

The study examined the different impacts of fuel usages on thermodynamic performances of a high bypass turbofan engine used in commercial aircraft. The study examined the PW4056 engine to observe the different fuel effects on the thermodynamic performance of a turbofan engine [12]. The energy, exergy, and sustainability analyses were performed on this engine. All analyses that was performed started at the same dead state conditions. In order to compare the different fuel performances for this engine, nineteen thermodynamic performance metrics were adapted for the purpose of this study. The overall study serves as a good reference to help improve the overall efficiency of a turbofan engine.

1.2.1.8 Turbofan Engine Health Assessment from Flight Data

This study examines the different approaches to engine health by using wing data from an engine of a commercial short-range aircraft obtained after a year of flight time. This was done by using an on-wing data measurements that analyzed three different approaches. In order to obtain good overall efficiency of a turbofan engine, a diagnostic process was used to track any engine deterioration. By taking this approach it helps reduce any issues to the engine or the engines health while in flight. Furthermore, this study provides good information that will serve as a good reference to help improve the overall efficiency of a turbofan engine.

1.2.1.9 Making Turbofan Engines More Energy Efficient

This study examined the different ways to making a turbofan engine more energy efficient. The study reviewed the different interaction and effects of cycle pressure ratio, firing temperature, bypass ratio, and component efficiencies on installed fuel consumption [13]. Also, the different possibilities for improvements in energy efficiency with operating economics and environmental characteristics are identified and reviewed. Parametric data was constructed which showed the trade-offs in the areas of efficiency and economics. Lastly, the balance of factors in cost effective advanced turbofans is discussed. This overall study serves as a good reference to help improve the overall efficiency of a turbofan engine.

1.2.2 Afterburner(s) Studies

1.2.2.1 Thermal Degradation of Turbine Components in A Military Turbofan

This study looked at the failure analysis of the turbine components of the RD-33 turbofan which is operated by the Polish Air Force. The thermal and dynamic stresses of the turbofan engine was analyzed. The study explained how the design of the afterburner activation system is a significant contributor to accelerated degradation of the turbine components and premature

grounding of engines [14]. It was mentioned that when the afterburner is activated, during the ignition and propagation of the flame, local overheating of the turbine components occurs and initiates their damage [15]. Furthermore, to combat this issue actions were proposed that would stop the negative impact of the afterburner. Overall, this study provides a well-developed approach to understanding how an afterburner work in regards to optimizing the overall efficiency of a turbofan engine.

1.2.2.2 Afterburner

This article gives an overview on how an afterburner works. The article examines how an afterburner is to provide a thrust increase. The article mentions that afterburning is normally achieved when the fuel is injected into a jet pipe downstream of the turbine. It was mentioned that; the advantage of afterburning is to significantly increased thrust; the disadvantage is its very high fuel consumption and inefficience [16]. Furthermore, this article gives a better understanding on how an afterburner works which will help optimize the overall efficiency of a turbofan engine for this report.

1.2.2.3 Afterburners. In: Aerothermodynamics of Aircraft Engine Components.

This book gives a general overview on how an afterburner works. This text went over the different characteristics of an afterburner. In addition to that, it explained the different flight conditions that an afterburner can be used under. The text explains the basic principles and concepts of propulsion combustion and goes over the different processes, limitations and analytical methods. Furthermore, this text book serves as a good reference for subject regarding afterburners.

1.2.3 Turbofan Engine While Incorporating an Afterburner(s) (Augmented Turbofan) Into Its Engine Cycle Studies

1.2.3.1 Propulsion and Power: An Exploration of Gas Turbine Performance Modeling

This text addresses the preliminary design of gas turbine engines, as well as the associated performance calculations. The text mentions how thermodynamics and turbomachinery is used throughout the design process for gas turbine engines. In addition to that, the text describes the background of augmented turbofan engines and their performances. Furthermore, this text is a good reference for the subject regarding augmented turbofan engines.

1.2.3.2 Developments in High-Speed Vehicle Propulsion Systems

This study explains the different technological achievements associated to the combined cycle engines such as the augmented turbofan engine. Some of the technologies that was described were the thermal management and how the afterburner was integrated with the turbofan engine. The study gave a better understanding on how the augmented turbofan propulsion systems are developed. Overall this study would be good reference for understanding how augmented turbofan engine is developed.

1.2.3.3 Aircraft Propulsion: Cleaner, Leaner, and Greener

This text examines the new technologies for propulsion and power, like turbofan propulsion systems. The text gave a thorough intro into the different innovations in aircraft gas turbine engines. These innovations evolved new engine concepts, and new vehicles an exploration of compressible flow with friction and heat, including a brief review of thermodynamics, isentropic process and flow, and conservation principles [17]. In addition to that, a discussion on gas turbine engine cycle analysis was given. This would in turn help with the design of the gas turbine engine cycle. Furthermore, this text provides information needed to get a better understanding on the different aircraft propulsion systems for this study.

1.2.3.4 Combustion in Advanced Gas Turbine Systems

This text looks at different design considerations in advanced gas turbine combustion chambers, combustion in industrial gas turbines, and the overall combustion cycle. The type of engine that the study was based on was the Rolls-Royce Spey engine. Discussions focus on mechanical condition, carbon-formation and exhaust smoke, system requirements, fuel oil ash deposition and corrosion, combustion-system design, performance requirements, types of primary zone, fuel injection, and combustion chamber types [18]. The text also explains subsonic flow flame holder studies using a low-pressure simulation technique and different augmentation systems for turbofan engines. Overall, this study provides a well-developed approach to understanding how a turbofan engine can incorporated an afterburner into its engine cycle.

1.3 Project Proposal

The objective of this project is to study and improve the overall efficiency of the turbofan engine while incorporating an afterburner(s) into its engine cycle for commercial airplanes. The main method of analysis would be done by using a computer software called GasTurb. This software will be used to simulate different gas turbines performance calculations and optimizations.

1.4 Methodology

Propulsion projects can be very expensive and requires a lot of time to design and manufacture. Therefore, a gas turbine software shall be used to analyze the performance and optimization calculations. The gas turbine software named GasTurb will be used to perform the necessary analyses for this study. The first step of the analysis will be to review and develop a turbofan engine geometry while including an afterburner. This will be done by researching a turbofan engine and its overall engine specifications. The specifications will involve the engines geometry, engine dimensions, compressor, combustor, and turbine. The different properties that would be researched are the freestream conditions (Mach Number, Temperature, Pressure) and Burner (Temperature). Furthermore, this step will help with the overall turbofan engine specifications.

The second step of the analysis is to do a steady state parametric cycle analysis for a turbofan engine while including an afterburner. The step will include a component analysis of the compressor, combustor, and turbine. Therefore, this step will help with the component analysis of the turbofan engine and afterburner.

The third step of the analysis is to do a computation analysis of the turbofan engine while integrating an afterburner using the gas turbine software; GasTurb. This step would define the computational framework of the turbofan engine. In addition to that, different simulations of the turbofan engine and the afterburner would be simulated under different constraints. Furthermore, this step will help with the computation analysis of the turbofan engine and afterburner.

Chapter 2 – Overview of the Turbofan Engine

2.1 The Turbofan Engine

Turbofan engines have been used as a means of propulsion for airplanes for over 8 decades. In the early years of development, the turbofan engine was not as fuel-efficient as it could have been. The reason for this is because their overall pressure ratio and turbine inlet temperature were severely limited by the technology and materials available at that time. However, as technology advanced throughout the years the turbofan engine is now one of the most fuel-efficient engines ever made. The turbofan is a portion of the turbine work used to supply power to the fan. Generally, the turbofan engine is more economical and efficient than the turbojet engine. The thrust specific fuel consumption is lower for turbofans and indicates a more economical operation. The turbofan also accelerates a larger mass of air to a lower velocity than a turbojet for a higher propulsive efficiency [19]. A schematic of a turbofan engine is shown in Figure 1.
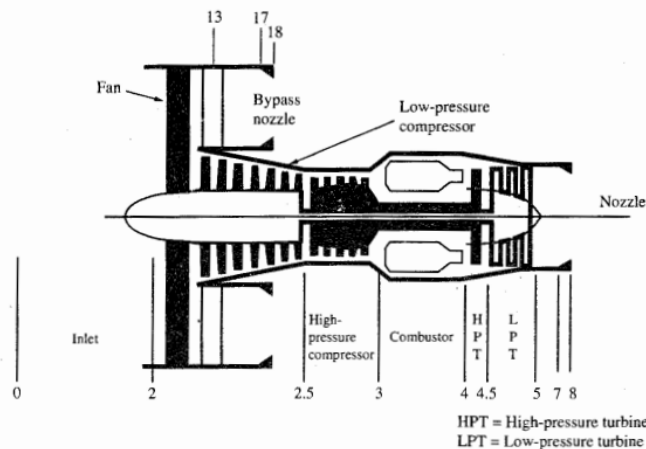
Figure 1. Schematic of a turbofan engine

The turbofan engine that will be studied for this report is the General Electric GE90-115B shown in Figure 2. The GE90-115B was developed from a list of General Electric GE90 turbofan engines. The GE90 engines is a family of high-bypass turbofan engines built by GE-Aviation for the Boeing 777, with thrust ranging from 74,000 to 115,000 lbf (329 to 512 kN). It was first introduced in November 1995 on British Airways' 777s, and is only available on the 777 [20]. In 1995, the GE90 engine debuted aboard a British Airways 777 airplane. Early GE90 engine models boasted outputs between 74,000 and 94,000 lbs. of thrust, and today it remains the world's largest turbofan engine. GE has continued to improve upon the GE90 design with larger variants such as the GE90 – 11B turbofan engine. This particular type of engine was built for Boeing's largest 777 models 777-200LR and 777-300ER. In 2005 the GE90-115B engine was selected to power the Boeing 777-300ER (2004), the Boeing 777-200LR Worldliner (2006) and

the Boeing 777 Freighter airplane. The GE90-115B 115,000-lb class engine was developed to meet the requirements of longer range Boeing 777-200LR and Boeing 777-300ER aircraft. It is considered as the world's most powerful jet engine and has set many world aviation records. It was developed in April of 2004 powering Air France's Boeing 777-300ER [21]. Table 1 lists the specifications for the GE90-115B turbofan engine.

Figure 2. GE90-115B turbofan engine

Table 1. Lists the specifications for the GE90-115B turbofan engine

Type	Dual rotor, axial flow, high bypass turbofan
Compressor	1 fan, 4-stage LP, 9-stage HP
Turbine	2-stage HP, 6-stage LP
Length	286.67 in (7.281 m)
Max. Width	148.38 in (3.769 m)
Max. Height	154.56 in (3.926 m)
Fan Diameter	128 in (3.3 m)
Weight	19,316 lb (8,762 kg)
Takeoff Thrust	110,760–115,540 lbf (492.7–513.9 kN)
LP Rotor Speed	2,355 rpm
HP Rotor Speed	9,332 rpm
Bypass ratio	9
Pressure ratio	42:1
Thrust-to-weight ratio	5.98

The turbofan engine has evolved from its introduction in the 1950s to its current role as the primary power source for today's commercial aviation fleet. A typical modern, high-bypass turbofan, shown in schematic cross-section in Figure 3, produces thrust to power aircraft by

ingesting ambient air, compressing the air, undergoing combustion, and expanding the hot gas through thrust-producing exhaust nozzles. As shown in the Figure 3, the incoming air flows into two streams: a fan stream and a primary stream. The flow of the fan stream also undergoes compression and expansion, but in this example stream expansion occurs only through the thrust-producing nozzle. The flow of the primary stream experiences compression and expansion, as the expansion process occurs both in the thrust-producing nozzle and, immediately upstream of the nozzle, in power-producing turbines that drive the compression systems of both streams [22]. This schematic gives a clear understanding how a turbofan engine work.
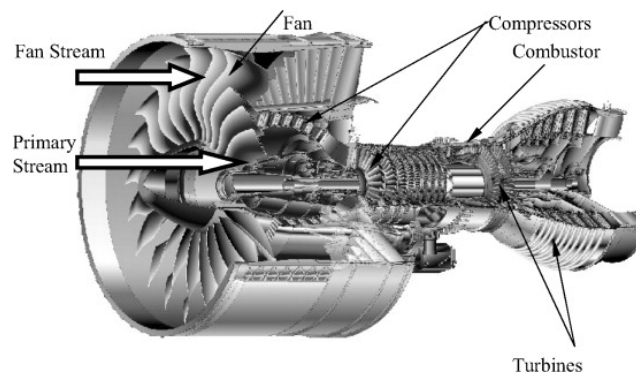
Figure 3. The cross-section of a high-bypass turbofan engine

2.2 The Turbofan Engine Compressor, Combustor and Turbine components

2.2.1 The Compressor

The function of the compressor is to increase the pressure of the incoming air so that the combustion process and the power extraction process after combustion can be carried out more efficiently. By increasing the pressure of the air, the volume of the air is reduced, which means that the combustion the fuel and air mixture will occur in a smaller volume [23].

GE90-115B turbofan engine is equip with a multistage axial compressor as shown in Figure 4. The way that the axial compressor works is that the air passes through in an axial direction through a series of rotating rotor blades and stationary stator vanes which are concentric with the axis of rotation. Each set of rotor blades and stator vanes is known as a stage. The flow path in an axial compressor decreases in the cross-sectional area in the direction of flow. The decrease of area is in proportion to the increased density of the air as the compression progresses from stage to stage. Each stage of an axial compressor produces a small compression

pressure ratio at a high efficiency. Therefore, for high pressure ratios with multiple compressors stages are used [24].
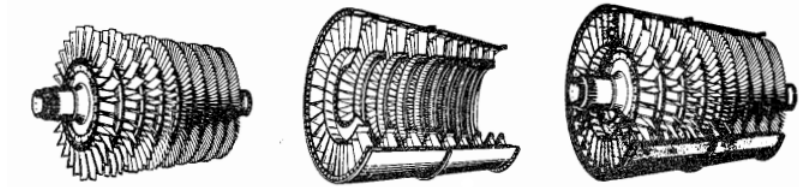
Figure 4. Multistage axial compressor

Therefore, the GE90-115B turbofan compressor is developed with low- and high-pressure compressors. In fact, there are four-stage low-pressure compressors and nine-stage high-pressure compressors as shown in Figure 5 and Figure 6. The purpose of the low-pressure compressor is to receive outside air from the fan and then compress the air to accelerate it through the engine. Afterwards, the air passes through the high-pressure compressors module that is made up of a series of rotor and stator assemblies. The main function of these assemblies is to raise the pressure of the air supplied to the combustor. The compressors have great compact engine construction and are made with rugged low aspect ratio airfoils. Therefore, the GE90-115B turbofan engine is equipped with compressors that will allow the engine to function correctly.
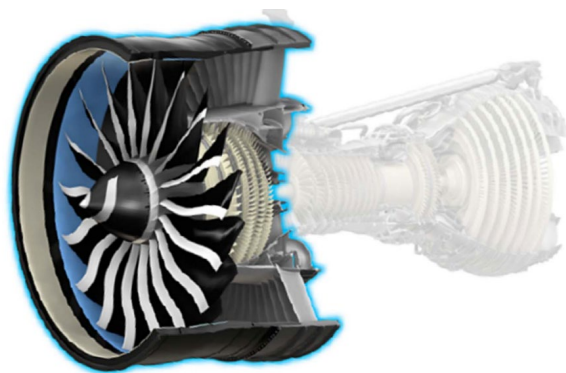
Figure 5. Low pressure compressors
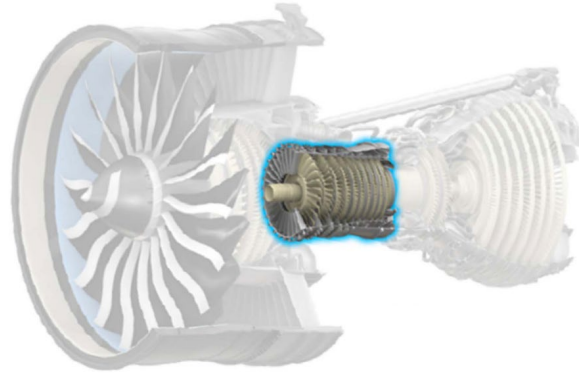
Figure 6. High pressure compressors

2.2.2 The Combustor

The combustor is designed to burn a mixture of fuel and air and to deliver the resulting gases to the turbine at a uniform temperature. The gas temperature must not exceed the allowable structural temperature of the turbine. A schematic of a combustor is shown in Figure 7 [25].
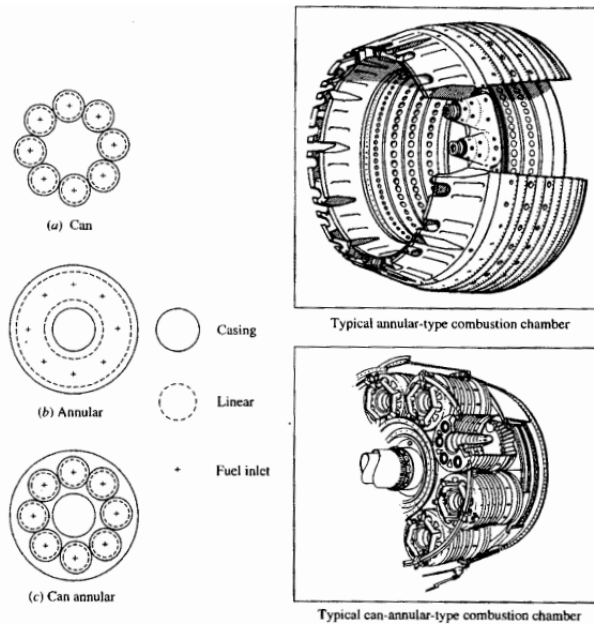
Figure 7. Schematic of a combustor

The combustor is where fuel is added to the cycle to create thermal energy. Most of today's modern turbofan engines employ an annular combustion system. The GE90-115B performance and efficiency, coupled with the GE90-115B dual annular combustor technology, significantly

limits fuel consumption and restricts hydrocarbon emissions to 40 percent of the level permitted by current international standards [26]. Figure 8 shows the location of the combustor on in GE90-115B.
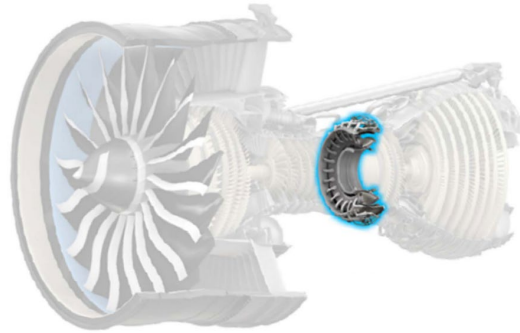
Figure 8. The combustor located in a GE90-115B turbofan engine

When it comes to turbofans engines, the combustor is where the additional energy is located to drive the turbines. In the combustor the liquid fuel is added to the flow which then flows to the fuel nozzles. When this happens, the temperature rises and then the turbofan cycle occurs as the fuel burns in the combustor. This is a site of significant heat transfer that must be accounted for in the design of the flow field. During the combustion process different changes occurs such as when the liquid fuel is vaporized before it combines with oxygen and releases the chemical energy that drives the turbofan cycle. The combustor is made to reduced NOX emission levels reduced unburned hydrocarbon, carbon monoxide and smoke levels [27]. In addition to that, the combustor has improved operability and a long-life liner construction. Therefore, the GE90-115B turbofan engine is equipped with a combustor that will allow the engine to function correctly.

2.2.3   The Turbine

The turbine extracts kinetic energy from the expanding gases which flow from the combustion chamber. The kinetic energy is converted to shaft horsepower to drive the compressor. The axial-flow turbine consists of a turbine wheel rotor and a set of stationary vanes stator, as shown in Figure 9. The set of stationary vanes of the turbine is a plane of vanes that are set at an angle to form a series of small nozzles which discharge the gases onto the blades of the turbine wheel. The discharge of the gases onto the rotor allows the kinetic energy of the gases to be transformed to mechanical shaft energy. Like the axial compressor, the axial turbine is usually multistage [28].
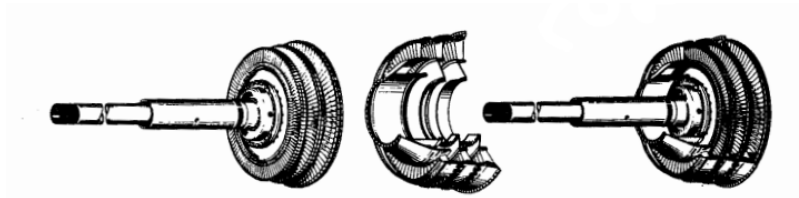
Figure 9. Axial-flow turbine components

Therefore, the when it comes to the GE90-115B turbofan, just as the compressor, it is developed with low-and high-pressure turbines. In fact, there are two-stage high-pressure turbines and six-stage low-pressure turbines as shown in Figure 10 and Figure 11. The purpose of the low-pressure turbine is to extract the remaining combustion thermal energy that drives the fan and low-pressure compressor rotor assembly. Afterwards, the air passes through the high-pressure turbine module that is made up of a high-pressure turbine rotor and nozzle guide vane assemblies, which extracts the combustion thermal energy that drives the high-pressure combustor. In addition to that, the turbine has a stiff supported rotor system which provides dynamic stability. It has a boltless assembly airfoil and shroud cooling circuits and also specialized film-cooled technology. Lastly, it is made with a multiple turbine cooling technology for better cooling effectiveness for the blades. Therefore, the GE90-115B turbofan engine is equipped with turbines that will allow the engine to function correctly.
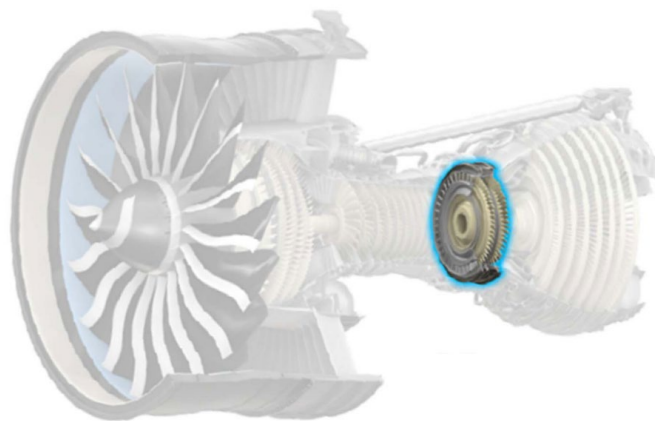
Figure 10. Two-stage high-pressure turbines
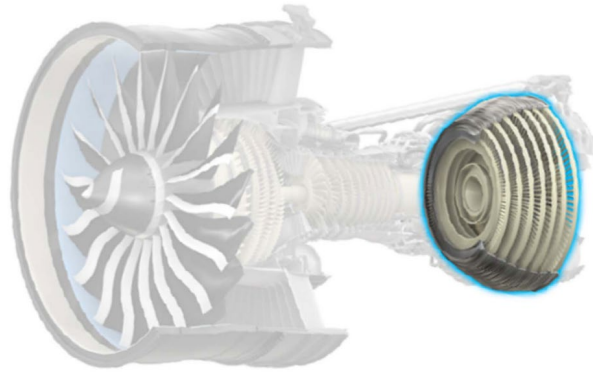
Figure 11. Six-stage low-pressure turbines

With all this in consideration, these turbofan engine components will be used to improve the overall efficiency of the turbofan engine cycle in this report. Therefore, the approach and procedures for this report will follow the different sources included to analyze and design a turbofan engine.

Chapter 3 – Governing Equations

There are multiple equations that governs the field of propulsion. For this report the governing equations will be in the area of Thermodynamics, Parametric Cycle Analysis of Ideal Engines, Component Performance, Parametric Cycle Analysis of Real Engines, Engine Performance Analysis and Inlets, Nozzles, and Combustion Systems. These areas of interest were picked from the textbook Elements of Gas Turbine Propulsion by Jack D. Mattingly. The governing equations were used to design the properties for the compressor, combustor and turbine for a turbofan engine with an afterburner.

The formulas that was used for the thermodynamics of the turbofan engine design was:

The Uninstalled Thrust F with a single inlet and single exhaust

V_0, V_e = velocities at inlet and exit

P_0, P_e = pressures at inlet and exit

$$F = \frac{(mdot_0 + mdot_f)V_e + mdot_0 V_o}{g_c} + (P_e + P_0)A_e \qquad (2.1)$$

The Uninstalled Thrust Equation

$$F = \frac{(mdot_0 + mdot_f)V_e - mdot_0 V_o}{g_c} \quad \text{for } P_e = P_o \tag{2.2}$$

The second performance parameter is the thrust specific fuel consumption (S and TSFC). This is the rate of fuel use by the propulsion system per unit of thrust produced. The uninstalled fuel consumption S and installed fuel consumption TSFC is written in equation form as;

$$S = \frac{mdot_f}{F} \tag{2.3}$$

$$TSFC = \frac{mdot_f}{T} \tag{2.4}$$

F = uninstalled thrust

S = uninstalled thrust specific fuel consumption

T = installed engine thrust

TSFC = installed thrust specific fuel consumption

$mdot_f$ = mass flow rate of fuel

The thermal efficiency of an engine is one useful engine performance parameter. Thermal efficiency is defined as the net rate of organized energy out of the engine which is then divided by the rate of thermal energy available from the fuel in the engine. The fuel's available thermal energy is equal to the mass flow rate of the fuel times the fuel heating value.

$$\eta_T = \frac{\dot{W}_{out}}{\dot{Q}_{in}} \tag{2.5}$$

n_T = thermal efficiency of engine

$Wdot_{out}$ = netpower out of engine

$Qdot_{in}$ = rate of thermal energy released

Propulsive efficiency is the ratio of the aircraft power to the power out of the engine as shown in the equation below.

$$\eta_P = \frac{TV_0}{\dot{W}_{out}}$$

(2.6)

where n_T = propulsive efficiency of engine

T = thrust of propulsion system

V_0 = velocity of aircraft

$Wdot_{out}$ = net power out of engine

The thermal and propulsive efficiencies can be combined to give the overall efficiency. When multiplying the propulsive efficiency by the thermal efficiency the overall efficiency of the propulsion system is formed as shown in the equation below.

$$\eta_O = \eta_P \eta_T$$

$$\eta_O = \frac{TV_0}{\dot{Q}_{in}}$$

(2.7)

The next set of equations are used to solve the parametric cycle analysis for ideal engines. The cycle analysis studies the thermodynamic changes of the working fluid as it flows through the engine. The parametric cycle analysis determines the performance of engines at different flight conditions arid values of design choice and design limit parameters [29].

In order to find the total/static temperature and pressure ratios of a free stream, the equations below are used. In addition to that, Table 2 was used to fine the temperature and pressure relationships for all τ and π values.

$$\tau_r = \frac{T_{t0}}{T_0} = 1 + \frac{\gamma - 1}{2} M_0^2$$

$$\pi_r = \frac{P_{t0}}{P_0} = \left(1 + \frac{\gamma - 1}{2} M_0^2\right)^{\gamma/(\gamma-1)}$$

(2.8)

17

Table 2. Temperature and pressure relationships for all τ and π.

Temperature and pressure relationships for all τ and π

Free stream		

$$\tau_r = 1 + \frac{\gamma - 1}{2}M_0^2 \qquad\qquad \pi_r = \left(1 + \frac{\gamma - 1}{2}M_0^2\right)^{\gamma/(\gamma-1)}$$

Core stream		Bypass stream	
$\tau_\lambda = \dfrac{c_{pt}T_{t4}}{c_{pc}T_0}$	$\tau_{\lambda AB} = \dfrac{c_{pAB}T_{t7}}{c_{pc}T_0}$	$\tau_{\lambda DB} = \dfrac{c_{pDB}T_{t17}}{c_{pc}T_0}$	
$\tau_d = \dfrac{T_{t2}}{T_{t0}}$	$\pi_d = \dfrac{P_{t2}}{P_{t0}}$	$\tau_f = \dfrac{T_{t13}}{T_{t2}}$	$\pi_f = \dfrac{P_{t13}}{P_{t2}}$
$\tau_c = \dfrac{T_{t3}}{T_{t2}}$	$\pi_c = \dfrac{P_{t3}}{P_{t2}}$	$\tau_{DB} = \dfrac{T_{t17}}{T_{t13}}$	$\pi_{DB} = \dfrac{P_{t17}}{P_{t13}}$
$\tau_b = \dfrac{T_{t4}}{T_{t3}}$	$\pi_b = \dfrac{P_{t4}}{P_{t3}}$	$\tau_{fn} = \dfrac{T_{t19}}{T_{t17}}$	$\pi_{fn} = \dfrac{P_{t19}}{P_{t17}}$
$\tau_t = \dfrac{T_{t5}}{T_{t4}}$	$\pi_t = \dfrac{P_{t5}}{P_{t4}}$		
$\tau_{AB} = \dfrac{T_{t7}}{T_{t5}}$	$\pi_{AB} = \dfrac{P_{t7}}{P_{t5}}$		
$\tau_n = \dfrac{T_{t9}}{T_{t7}}$	$\pi_n = \dfrac{P_{t9}}{P_{t7}}$		

Table 3 shows the summary of equations that was used for an ideal turbofan engine. These equations were also used to solve the parametric cycle analysis for ideal turbofan engines.

Table 3. Summary of equations - ideal turbofan

Summary of Equations—Ideal Turbofan

INPUTS: $M_0,\ T_0(K, {}^\circ R),\ \gamma,\ c_p\left(\dfrac{kJ}{kg \cdot K}, \dfrac{Btu}{lbm \cdot {}^\circ R}\right), h_{PR}\left(\dfrac{kJ}{kg}, \dfrac{Btu}{lbm}\right),$
$T_{t4}(K, {}^\circ R),\ \pi_c,\ \pi_f,\ \alpha$

OUTPUTS: $\dfrac{F}{\dot{m}_0}\left(\dfrac{N}{kg/sec}, \dfrac{lbf}{lbm/sec}\right), f,\ S\left(\dfrac{mg/sec}{N}, \dfrac{lbm/hr}{lbf}\right), \eta_T,\ \eta_P,\ \eta_O,\ FR$

EQUATIONS:

$R = \dfrac{\gamma - 1}{\gamma}c_p$

$a_0 = \sqrt{\gamma R g_c T_0}$

$\tau_r = 1 + \dfrac{\gamma - 1}{2}M_0^2$

$\tau_\lambda = \dfrac{T_{t4}}{T_0}$

$\tau_c = (\pi_c)^{(\gamma-1)/\gamma}$

$\tau_f = (\pi_f)^{(\gamma-1)/\gamma}$

$\dfrac{V_9}{a_0} = \sqrt{\dfrac{2}{\gamma - 1}\left\{\tau_\lambda - \tau_r[\tau_c - 1 + \alpha(\tau_f - 1)] - \dfrac{\tau_\lambda}{\tau_r \tau_c}\right\}}$

$\dfrac{V_{19}}{a_0} = \sqrt{\dfrac{2}{\gamma - 1}(\tau_r \tau_f - 1)}$

$\dfrac{F}{\dot{m}_0} = \dfrac{a_0}{g_c}\dfrac{1}{1 + \alpha}\left[\dfrac{V_9}{a_0} - M_0 + \alpha\left(\dfrac{V_{19}}{a_0} - M_0\right)\right]$

$f = \dfrac{c_p T_0}{h_{PR}}(\tau_\lambda - \tau_r \tau_c)$

$S = \dfrac{f}{(1 + \alpha)(F/\dot{m}_0)}$

$\eta_T = 1 - \dfrac{1}{\tau_r \tau_c}$

$\eta_P = 2M_0\dfrac{V_9/a_0 - M_0 + \alpha(V_{19}/a_0 - M_0)}{V_9^2/a_0^2 - M_0^2 + \alpha(V_{19}^2/a_0^2 - M_0^2)}$

$\eta_O = \eta_T \eta_P$

$FR = \dfrac{V_9/a_0 - M_0}{V_{19}/a_0 - M_0}$

Following the equations mentioned above, the rest of the report uses equations and concepts from chapters Component Performance, Parametric Cycle Analysis of Real Engines, Engine Performance Analysis and Inlets, Nozzles, and Combustion Systems. These concepts will be used to design the properties for the compressor, combustor and turbine for a turbofan engine with an afterburner.

Chapter 4 – Theory

4.1 The Brayton Cycle

The Brayton power cycle is a model used in thermodynamics. This cycle can be used for an ideal gas turbofan engine. The Brayton cycle consists of four different thermodynamic processes.

1) The Isentropic Compression Process (From 2 to 3)
2) The Constant-Pressure Head Addition Process (From 3 to 4)
3) The Isentropic Expansion Process (From 4 to 9)
4) The Constant-Pressure Head Rejection Process (From 9 to 2)

Figure 12 shows a pictorial example of the Brayton cycle, which includes a TS-diagram and its four different thermodynamic processes.
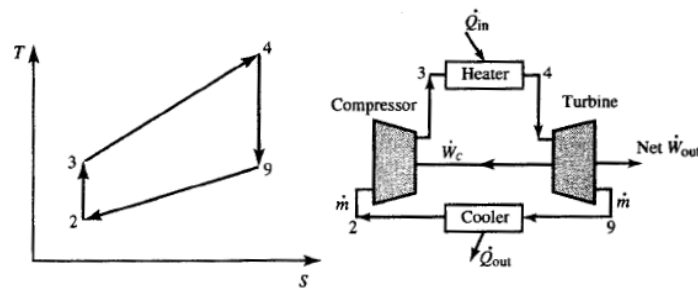
Figure 12. The Brayton cycle which includes a TS-diagram

For the Brayton cycle when the process starts and goes through the compressor and then the turbine it is considered to be reversible and adiabatic which is an isentropic process. In addition to that, when the process passes through the heater and cooler, it is considered to be the constant-pressure process of the Brayton cycle. When the Brayton cycle passes through both the compressor and the turbine it is considered to be reversible and adiabatic (isentropic). For the process that goes through the heater and cooler is considered to be constant-pressure [30].

19

For a calorically perfect gas, the Brayton cycle yields a set of equations listed below, for the rate of energy transfer through each engine component.

$$\dot{W}_c = \dot{m}c_p(T_3 - T_2) \qquad \dot{Q}_{in} = \dot{m}c_p(T_4 - T_3)$$
$$\dot{W}_t = \dot{m}c_p(T_4 - T_9) \qquad \dot{Q}_{out} = \dot{m}c_p(T_9 - T_2)$$
$$\text{Net } \dot{W}_{out} = \dot{W}_t - \dot{W}_c = \dot{m}c_p[T_4 - T_9 - (T_3 - T_2)]$$

(4.1)

From these equations the thermal efficiency for the Brayton cycle is derived. Equation 4.2 is the thermal efficiency equation for a Brayton cycle.

$$\eta_T = 1 - \left(\frac{1}{PR}\right)^{(\gamma-1)/\gamma}$$

(4.2)

Since the engine that's going to be modeled for this report has an afterburner, Figure 13 shows a pictorial example of the Brayton cycle with an afterburner, which includes a TS-diagram and its different thermodynamic processes.
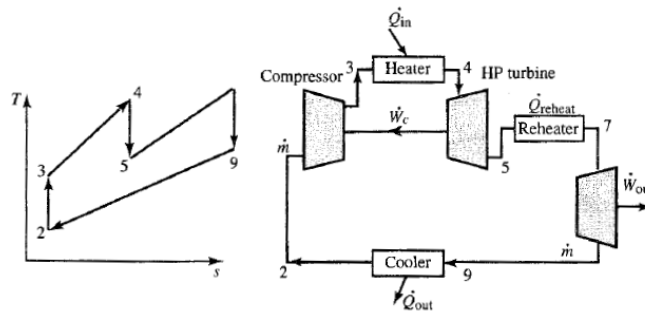
Figure 13. The Brayton cycle with an afterburner which includes a TS-diagram

Figure 13 shows the Brayton cycle with reheat. The addition of reheat to the cycle increases the specific power of the free turbine and reduces the thermal efficiency [31]. The cycle analysis studies the different thermodynamic changes of the working fluid as it flows through the engine. It is divided into two types of analysis: parametric cycle analysis and engine performance analysis. Parametric cycle analysis determines the performance of engines at different flight conditions arid values of design choice and design limit parameters. Engine performance analysis determines the performance of a specific engine at all flight conditions and throttle settings [32].

20

The main objective of the parametric cycle analysis is to relate the engine performance parameters to the design choices, the design limitations, and the flight environment. From the parametric cycle analysis, it can easily be determined which engine type and component design characteristics best satisfy a particular need. In other words, the parametric cycle analysis will relate the engine performance parameters such as the thrust and thrust specific fuel consumption, the design choices such as the compressor pressure ratio, bypass ratio, etc. the design limitations such as the burner exit temperature, compressor exit pressure, etc. and lastly the flight environment such as the Mach number, ambient temperature, etc. From these parameters the parametric cycle analysis can determine what the engine type would be such as a turbojet or turbofan engine and the component design characteristics such as the range of the aircraft flight. Therefore, the realistic values from this cycle analysis can help design a realistic turbofan engine.

4.2 The Steps of the Parametric Cycle Analysis Process

The general steps that would be used in order to perform a steady state parametric cycle analysis for a turbofan engine with an afterburner for mixed exhaust streams would be the steps from the engine parametric cycle analysis for a jet engine with a single inlet and single exhaust. Figure 14 is a gas turbine engine with station numbering, which will be used to analysis the turbofan engine flows.
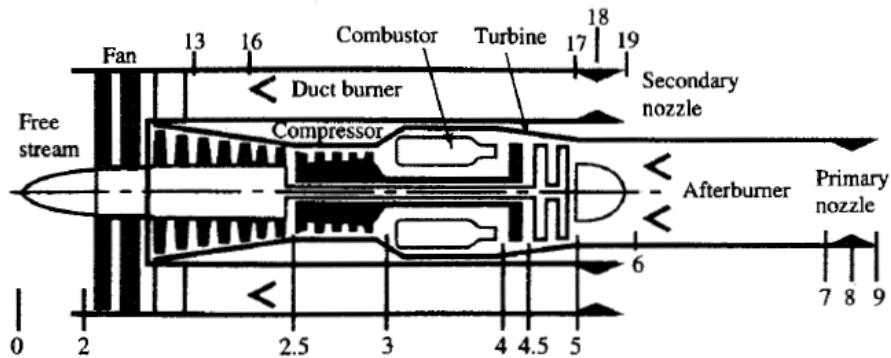
Figure 14. A gas turbine engine with station numbering

The following steps are used to perform a steady state parametric cycle analysis.

Step 1 starts with an equation for uninstalled engine thrust. The equations that was used was in terms of the total pressure and total temperature ratios, the ambient pressure P_0, temperature T_0, speed of sound a_0, and the Mach number M_0. The equations derived from this step are:

$$F = \frac{1}{g_c}(\dot{m}_9 V_e - \dot{m}_0 V_0) + A_9(P_9 - P_0)$$

$$\frac{F}{\dot{m}_0} = \frac{a_0}{g_c}\left(\frac{\dot{m}_9}{\dot{m}_0}\frac{V_9}{a_0} - M_0\right) + \frac{A_9 P_9}{\dot{m}_0}\left(1 - \frac{P_0}{P_9}\right)$$

(4.3)

Step 2 uses equation 4.4 for the velocity ratio V_9/a_0 in terms of Mach numbers, temperatures, and gas properties.

$$\left(\frac{V_9}{a_0}\right)^2 = \frac{a_9^2 M_9^2}{a_0^2} = \frac{\gamma_9 R_9 g_c T_9}{\gamma_0 R_0 g_c T_0} M_9^2$$

(4.4)

Step 3 uses the set of equations to find the exit Mach number M_9 of the engine.

$$P_{t9} = P_9\left(1 + \frac{\gamma - 1}{2} M_9^2\right)^{\gamma/(\gamma-1)}$$

$$M_9^2 = \frac{2}{\gamma - 1}\left[\left(\frac{P_{t9}}{P_9}\right)^{(\gamma-1)/\gamma} - 1\right]$$

$$\frac{P_{t9}}{P_9} = \frac{P_0}{P_9}\frac{P_{t0}}{P_0}\frac{P_{t2}}{P_{t0}}\frac{P_{t3}}{P_{t2}}\frac{P_{t4}}{P_{t3}}\frac{P_{t5}}{P_{t4}}\frac{P_{t7}}{P_{t5}}\frac{P_{t9}}{P_{t7}}$$

$$= \frac{P_0}{P_9}\pi_r\pi_d\pi_c\pi_b\pi_t\pi_{AB}\pi_n$$

(4.5)

Step 4 uses the set of equations to find the temperature ratio T_9/T_0 of the engine.

$$\frac{T_9}{T_0} = \frac{T_{t9}/T_0}{T_{t9}/T_9} = \frac{T_{t9}/T_0}{(P_{t9}/P_9)^{\gamma-1)/\gamma}}$$

$$\frac{T_{t9}}{T_0} = \frac{T_{t0}}{T_0}\frac{T_{t2}}{T_{t0}}\frac{T_{t3}}{T_{t2}}\frac{T_{t4}}{T_{t3}}\frac{T_{t5}}{T_{t4}}\frac{T_{t7}}{T_{t5}}\frac{T_{t9}}{T_{t7}} = \tau_r\tau_d\tau_c\tau_b\tau_t\tau_{AB}\tau_n$$

(4.6)

Step 5 uses the first law of thermodynamics which is applied to the combustor to find an expression for the fuel/air ratio for an engine.

$$\dot{m}_0 c_p T_{t3} + \dot{m}_f h_{PR} = \dot{m}_0 c_p T_{t4}$$

<div align="right">(4.7)</div>

Step 6 uses Step 5 to find the expression for the total temperature ratio across the turbine T_t. To do this one has to relate the turbine power output to the compressor and fan power requirements.

Step 7 would be to evaluate the specific thrust from the above results.

Step 8 uses the thrust specific fuel consumption to evaluate the results for the specific thrust and fuel/air ratio. Equation 4.8 is the specific thrust and fuel/air ratio.

$$S = \frac{f}{F/\dot{m}_0}$$

<div align="right">(4.8)</div>

Step 9 is to develop the different expressions for the thermal and propulsive efficiencies of the engine.

Furthermore, these steps will be used as a guide to analyze the parametric cycle analysis for real engines. Following the equations mentioned above; the next chapter of this report will cover the analysis using the parametric cycle analysis for real engines. The equations and concepts will be used to design the properties for the compressor, combustor and turbine for a turbofan engine with an afterburner.

Chapter 5 – A Steady State Parametric Cycle Analysis for a Turbofan Engine with an Afterburner for Mixed Exhaust Streams

5.1 The Steady State Parametric Cycle Analysis for a Turbofan Engine with an Afterburner for Mixed Exhaust Streams

Following the steps from chapter 4 for analyzing an engine using the parametric cycle analysis; chapter 5 will use the same steps described in chapter 4 however, for a turbofan engine with an afterburner for mixed exhaust streams. A realistic approach will be taken to analyze this type of engine. The parametric cycle analysis of a turbofan engine with an afterburner will be developed in steps. First the general steps applicable to the parametric cycle analysis for engines will be introduced. Next these steps will be used to analyze the engine components, the different trends that is produced and the performance trends.

5.2 The Design Inputs

When solving the steady state parametric cycle analysis for a turbofan engine with an afterburner for mixed exhaust streams the total temperature ratios, total pressure ratios, etc. will be classified into four categories:

1. Flight Conditions P_0, T_0, M_0, c_p, T_r, π_r
2. Design Limits $(c_p T_t)_{\text{burner exit}}$
3. Components Performance π_d, π_b, π_n, etc.
4. Design Choices π_c, π_f, etc.

From these four categories the temperature and pressure relationships for all T and π are shown in Table 4.

Table 4. Temperature and pressure relationships for all τ and π.

Temperature and pressure relationships for all τ and π

	Free stream		
$\tau_r = 1 + \dfrac{\gamma-1}{2}M_0^2$		$\pi_r = \left(1 + \dfrac{\gamma-1}{2}M_0^2\right)^{\gamma/(\gamma-1)}$	
Core stream		**Bypass stream**	

Core stream		Bypass stream	
$\tau_\lambda = \dfrac{c_{pt}T_{t4}}{c_{pc}T_0}$	$\tau_{\lambda AB} = \dfrac{c_{pAB}T_{t7}}{c_{pc}T_0}$	$\tau_{\lambda DB} = \dfrac{c_{pDB}T_{t17}}{c_{pc}T_0}$	
$\tau_d = \dfrac{T_{t2}}{T_{t0}}$	$\pi_d = \dfrac{P_{t2}}{P_{t0}}$	$\tau_f = \dfrac{T_{t13}}{T_{t2}}$	$\pi_f = \dfrac{P_{t13}}{P_{t2}}$
$\tau_c = \dfrac{T_{t3}}{T_{t2}}$	$\pi_c = \dfrac{P_{t3}}{P_{t2}}$	$\tau_{DB} = \dfrac{T_{t17}}{T_{t13}}$	$\pi_{DB} = \dfrac{P_{t17}}{P_{t13}}$
$\tau_b = \dfrac{T_{t4}}{T_{t3}}$	$\pi_b = \dfrac{P_{t4}}{P_{t3}}$	$\tau_{fn} = \dfrac{T_{t19}}{T_{t17}}$	$\pi_{fn} = \dfrac{P_{t19}}{P_{t17}}$
$\tau_t = \dfrac{T_{t5}}{T_{t4}}$	$\pi_t = \dfrac{P_{t5}}{P_{t4}}$		
$\tau_{AB} = \dfrac{T_{t7}}{T_{t5}}$	$\pi_{AB} = \dfrac{P_{t7}}{P_{t5}}$		
$\tau_n = \dfrac{T_{t9}}{T_{t7}}$	$\pi_n = \dfrac{P_{t9}}{P_{t7}}$		

5.3 The Turbofan Engine with an Afterburner for Mixed Exhaust Streams

The figure 15 below is a cross section of a mixed-flow afterburning turbofan engine. This engine cycle is used on many aircraft engines. This engine cycle has several advantages over the turbofan engine with separate exhausts; one is that it has one variable-area exhaust nozzle, two it has one augmenter afterburner, and three it has cold bypass air to cool the afterburner liner.
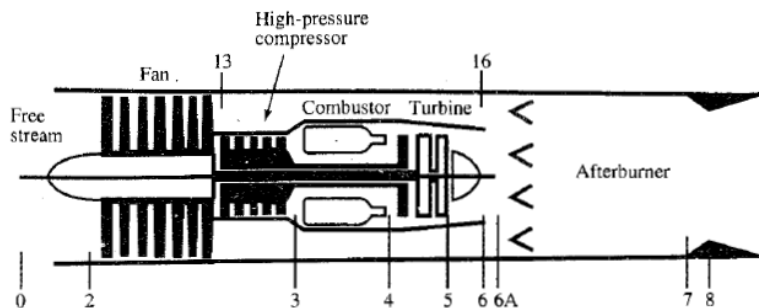
Figure 15. A cross section of a mixed-flow afterburning turbofan engine

Since this engine is a mixed-flow afterburning turbofan engine it has to have a mixer to pass the streams through. Figure 16 is an example of a mixer which has a bypass-stream and a core

stream. These two streams allow air to pass through the engine and into the mixer. Once these two streams pass through the mixer it becomes a mixed stream.
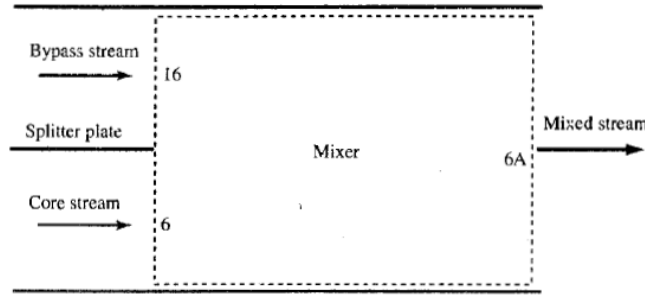
Figure 16. A mixer that has a bypass-stream and a core stream

The mixed stream flows can lead to different parameters which can be used to analyze a mixed-flow afterburning turbofan engine such as the total temperature and pressure ratios, Mach numbers, mass flow rates, mass flow parameters, etc. Lastly, these parameters are then used to solve the conservation of mass, conservation of energy, momentum and constant area of a turbofan engine.

5.4 The Steps for Solving A Turbofan Engine with an Afterburner for Mixed Exhaust Streams

This section of the chapter develops the equations needed to analyze the mixed flow afterburning turbofan engine. For this particular turbofan engine, it can use the uninstalled thrust equation 5.1.

$$F = \frac{1}{g_c}(\dot{m}_9 V_9 - \dot{m}_0 V_0) + A_9(P_9 - P_0)$$

$$\frac{F}{\dot{m}_0} = \frac{a_0}{g_c}\left(\frac{\dot{m}_9}{\dot{m}_0}\frac{V_9}{a_0} - M_0\right) + \frac{A_9 P_9}{\dot{m}_0}\left(1 - \frac{P_0}{P_9}\right)$$

(5.1)

From this equation, the expression for the overall fuel/air ratio for this engine is the total fuel flow rate divided by the inlet airflow rate.

$$f_O = \frac{\dot{m}_f + \dot{m}_{fAB}}{\dot{m}_0}$$

(5.2)

For this analysis it is assumed that the mass flow rate at station 9 equals the mass flow rate at station 0 plus the fuel added in the main burner and in the afterburner. Therefore, equation 5.3 is formed from equation 5.2.

$$\dot{m}_9 = \dot{m}_0 + \dot{m}_f + \dot{m}_{fAB}$$

$$\frac{\dot{m}_9}{\dot{m}_0} = 1 + f_O$$

(5.3)

The equations mentioned above are used as the foundation to analyze the mixed flow afterburning turbofan engine. The following 8 steps will be used to analyze this afterburning turbofan engine.

Step 1 is to solve the uninstalled thrust of the turbofan engine. The equations mentioned above is used to form the uninstalled thrust equation.

$$\frac{F}{\dot{m}_0} = \frac{a_0}{g_c} \left[(1 + f_O) \frac{V_9}{a_0} - M_0 + (1 + f_O) \frac{R_9}{R_c} \frac{T_9/T_0}{V_9/a_0} \frac{1 - P_0/P_9}{\gamma_c} \right]$$

(5.4)

Step 2 is to solve the velocities at stations 0 and 9. The equations 5.5 and 5.6 are used to solve the velocities.

$$\left(\frac{V_9}{a_0} \right)^2 = \frac{a_9^2 M_9^2}{a_0^2} = \frac{\gamma_9 R_9 g_c T_9}{\gamma_0 R_0 g_c T_0} M_9^2$$

(5.5)

$$\left(\frac{V_9}{a_0} \right)^2 = \frac{\gamma_9 R_9 T_9}{\gamma_c R_c T_0} M_9^2$$

(5.6)

Step 3 is used to solve the Mach number and total pressures at station 9. Equations 5.7 are used to solve the Mach number and total pressures.

$$M_9^2 = \frac{2}{\gamma_9 - 1} \left[\left(\frac{P_{t9}}{P_9} \right)^{(\gamma_9 - 1)/\gamma_9} - 1 \right]$$

$$\frac{P_{t9}}{P_9} = \frac{P_0}{P_9} \pi_r \pi_d \pi_c \pi_b \pi_t \pi_M \pi_{AB} \pi_n$$

(5.7)

27

Step 4 is to solve the total temperature at stations 0 and 9. Equation 5.8 is used to solve the total temperature when the afterburner is on and off during flight.

$$\frac{T_9}{T_0} = \frac{T_{t9}/T_0}{(P_{t9}/P_9)^{(\gamma_9-1)/\gamma_9}}$$

$$T_{t9} = T_{t4}\tau_t\tau_M \qquad \text{afterburner off}$$

$$T_{t9} = T_{t7} \qquad \text{afterburner on}$$

(5.8)

Step 5 applies the first law of thermodynamics to the main burner. Equation 5.9 applies the first law of thermodynamics to the afterburner. From that equation it is then divided by $m_0 C_{pc} T_0$ and using the different definitions of temperature ratios yields equation 5.10. Lastly, equation 5.11 is formed by using equations 5.9 and 5.10 to solve the afterburner fuel/air ratio for the turbofan engine.

$$\dot{m}_{6A} c_{p6A} T_{t6A} + \eta_{AB}\dot{m}_{fAB}h_{PR} = \dot{m}_7 c_{p7} T_{t7}$$

(5.9)

$$\left(1 + \frac{f}{1+\alpha}\right)\frac{c_{p6A}}{c_{pt}}\tau_\lambda\tau_t\tau_M + f_{AB}\frac{\eta_{AB}h_{PR}}{c_{pc}T_0} = \left(1 + \frac{f}{1+\alpha} + f_{AB}\right)\tau_{\lambda AB}$$

(5.10)

$$f_{AB} = \left(1 + \frac{f}{1+\alpha}\right)\frac{\tau_{\lambda AB} - (c_{p6A}/c_{pt})\tau_\lambda\tau_t\tau_M}{\eta_{AB}h_{PR}/(c_{pc}T_0) - \tau_{\lambda AB}}$$

(5.11)

Step 6 is to solve the power balance between the turbine, compressor, and fan with a mechanical efficiency of the turbine shaft. Equation 5.12 is then formed to solve the turbine temperature ratio.

$$\tau_t = 1 - \frac{1}{\eta_m(1+f)}\frac{\tau_r}{\tau_\lambda}[\tau_c - 1 + \alpha(\tau_f - 1)]$$

(5.12)

Equation 5.13 is used to make sure that the total pressures at stations 6 and 16 remain equal. When assuming isentropic flow in the bypass duct from stations 13 to 16 equation 5.13 is formed.

$$\tau_t = \pi_t^{(\gamma_t-1)e_t/\gamma_t} = \left(\frac{\pi_f}{\pi_c \pi_b}\right)^{(\gamma_t-1)e_t/\gamma_t}$$

(5.13)

Lastly, equations 5.12 and 5.13 can be used to solved the bypass ratio α of the fan temperature ratio T_f in terms of the known quantities. The bypass ratio solution yields equation 5.14.

$$\alpha = \frac{\eta_m(1+f)(\tau_\lambda/\tau_r)\{1 - [\pi_f/(\pi_c\pi_b)]^{(\gamma_t-1)e_t/\gamma_t}\} - (\tau_c - 1)}{\tau_f - 1}$$

(5.14)

Step 7 uses equation 5.15 to solve the thrust specific fuel consumption for the turbofan engine.

$$S = \frac{f_O}{F/\dot{m}_0}$$

(5.15)

Step 8 uses equations 5.16 to solve the propulsive and thermal efficiency for the turbofan engine.

$$\eta_P = \frac{2g_c V_0(F/\dot{m}_0)}{a_0^2[(1+f_O)(V_9/a_0)^2 - M_0^2]}$$

$$\eta_T = \frac{a_0^2[(1+f_O)(V_9/a_0)^2 - M_0^2]}{2g_c f_O h_{PR}}$$

(5.16)

The 8 steps mentioned above will be used to analyze the mixed-flow afterburning turbofan engine with mixed exhaust streams. The next chapter of this report will cover the analysis done using the parametric cycle analysis for real engines. The equations and concepts from this report will be used to design the properties for the compressor, combustor and turbine for a turbofan engine with an afterburner.

Chapter 6 – A Parametric Cycle Analysis for a 2 Spool Mixed Turbofan Engine with an Afterburner Using GasTurb Software

6.1 A Parametric Cycle Analysis for a 2 Spool Mixed Turbofan Engine with an Afterburner Using GasTurb Software

This chapter of the report will go over the process used to obtain the values for a 2 spool mixed turbofan engine with an afterburner using the GasTurb as the main software package. GasTurb is a gas turbine performance calculation and optimization program. It simulates most of the gas turbine configurations in use for propulsion or for power generation. Therefore, a basic understanding of turbofan engine performance calculations was used to make best use of this software. The software was used to conduct a design point calculation using a turbofan engine with an afterburner. Also, it was used to calculate basic thermodynamics properties for a turbofan engine. Next, the software was used to calculate a gas turbine cycle using the design point calculation, the enthalpy-entropy diagram (H-S diagram), the temperature-entropy (T-S diagram) and the pressure-volume (P-V diagram). The design parametric study such as the use of conducting parametric studies, contours and design Limits. Then the off-design simulations such as the use of off-design point calculation, usage of component maps, and the usage of operating lines to view different graphs. Lastly, the design of the engine geometry was determined.

6.2 A Parametric Cycle Analysis for a 2 Spool Mixed Turbofan Engine with an Afterburner

The 2 spool mixed turbofan engine with an afterburner design configuration will be used for this study. The input data for a 2 spool mixed turbofan engine with an afterburner were generated by the GasTurb software. The most important input design parameters are listed in Table 5 below. The parameters such as the Burner Exit Temperature and the Mixer Efficiency played an important role when it came to the overall efficiency of the turbofan engine.

Table 5. Input Design Parameters

Property	Unit	Value	Comment
Intake Pressure Ratio		-0.99	
No (0) or Average (1) Core dP/P		1	
Inner Fan Pressure Ratio		2.5	
Booster Map Type (0/1/2)		0	used for off design only
Outer Fan Pressure Ratio		3	
Compr. Interduct Press. Ratio		0.99	
HP Compressor Pressure Ratio		7	
Bypass Duct Pressure Ratio		0.97	
Turb. Interd. Ref. Press. Ratio		0.98	
Design Bypass Ratio		1	
Burner Exit Temperature	K	1600	
Burner Design Efficiency		0.9995	
Burner Partload Constant		1.6	used for off design only
Fuel Heating Value	MJ/kg	43.124	
Overboard Bleed	kg/s	0	
Power Offtake	kW	50	
HP Spool Mechanical Efficiency		1	
LP Spool Mechanical Efficiency		1	
Burner Pressure Ratio		0.97	
Turbine Exit Duct Press Ratio		0.98	
Hot Stream Mixer Press Ratio		0.99	
Cold Stream Mixer Press Ratio		0.99	
Mixed Stream Pressure Ratio		1	
Mixer Efficiency		0.5	
Design Mixer Mach Number		0.247	
Design Mixer Area	m²	0	

The Burner Exit Temperature is 1,600K and the Mixer Efficiency is 0.5. The ambient conditions for the turbofan engine had a Mach number of 1.5 and had flight altitude of 11,000m. The Mach number and flight altitude came from the standard atmosphere, which was used to define the inlet conditions of the turbofan engine. Alternatively, the ambient pressure and the total pressure and temperature at the engine inlet was directly specified.

The stations of the 2 spool mixed turbofan engine with an afterburner will now be examine next. The stations of the 2 spool mixed turbofan engine with an afterburner are labelled in accordance with SAE notation as shown in Figure 17 below.
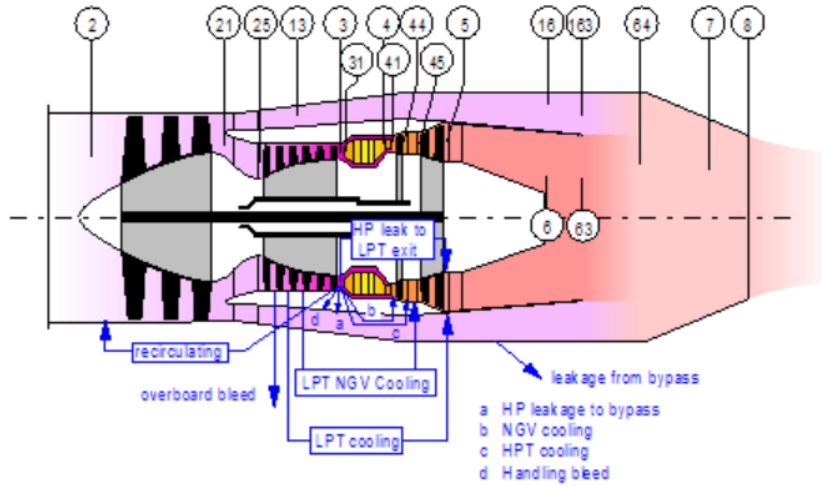
Figure 17. A 2 spool mixed turbofan engine with an afterburner labelled with sae notation

The flow areas at the stations were derived from the Mach number. The flow areas influence the calculated static pressures and temperatures but do not affect main cycle parameters such as the thermal efficiency or thrust. There are several more input options such as the secondary air system, the compressor, the turbine, the reheat system and the nozzle all played an important role with the afterburner staying efficient.

Next, the design point calculation was done. For this part all of the input data with the predefined values was left the same. Once the calculation was completed, the results of the simulation is shown in Table 6 below.

Table 6. Design point calculations for the 2 spool mixed turbofan engine

```
           W         T         P      WRstd
Station   kg/s       K        kPa      kg/s          FN       =    12.87 kN
 amb               216.65    22.632
   1      37.741   314.28    83.127                  TSFC     =    30.6770 g/(kN*s)
   2      37.741   314.28    79.875    50.000        WF Burner=     0.39468 kg/s
  13      18.870   444.88   239.624     9.915        s NOX    =     0.6828
  21      18.870   433.98   199.687    11.751        BPR      =     1.0000
  25      18.870   433.98   197.690    11.870        Core Eff =     0.5556
   3      18.304   788.36  1383.830     2.217        Prop Eff =     0.7257
  31      16.323   788.36  1383.830                  P3/P2    =    17.325
   4      16.718  1600.00  1342.315     2.974
  41      17.661  1560.09  1342.315     3.102        P16/P6   =     1.34862
  43      17.661  1241.89   439.213                  A63      =     0.30047 m²
  44      18.605  1220.48   439.213                  A163     =     0.04715 m²
  45      18.605  1220.48   430.429     9.013        A64      =     0.34763 m²
  49      18.605  1006.72   175.868                  XM63     =     0.17704
   5      19.171   996.89   175.868    20.544        XM163    =     0.69271
   6      19.171   996.89   172.351                  XM64     =     0.24700
  16      18.870   444.88   232.435                  P63/P6   =     0.99000
  64      38.041   735.27   181.219                  P163/P16 =     0.99000
   8      38.041   735.27   181.219    33.977        A8       =     0.14971 m²
 Bleed     0.094   788.36  1383.823                  CD8      =     0.95000
-----------------------------------------------     Ang8     =    25.00 °
Efficiencies:  isentr  polytr   RNI    P/P|          P8/Pamb  =     8.00720
 Outer LPC     0.8800  0.8967  0.711  3.000          WLkBy/W25=     0.00000
 Inner LPC     0.7800  0.8060  0.711  2.500          WCHN/W25 =     0.05000
 HP Compressor 0.8600  0.8908  1.198  7.000          WCHR/W25 =     0.05000
 Burner        0.9995                 0.970          Loading  =   100.00 %
 HP Turbine    0.9000  0.8876  1.842  3.056          WCLN/W25 =     0.00000
 LP Turbine    0.9100  0.9007  0.783  2.447          WCLR/W25 =     0.03000
 Mixer         0.5000                                WBHD/W21 =     0.00000
-----------------------------------------------     far7     =     0.01048
HP Spool mech Eff 1.0000  Nom Spd  22800 rpm         WBLD/W25 =     0.00500
LP Spool mech Eff 1.0000  Nom Spd  14600 rpm         PWX      =    50.0 kW
-----------------------------------------------     P16/P13  =     0.9700
P2/P1= 0.9609 P25/P21=0.9900 P45/P44= 0.9800         P6/P5    =     0.9800
```

32

Table 6 is a summary that shows the thermodynamic details regarding the states in the stations of the turbofan engine. All parameters are abbreviated in accordance with international standard nomenclature. The details at the thermodynamic stations will be examined. For every station of the gas turbine all the thermodynamic parameters are listed as shown in Table 6. The calculated values for the areas are listed as well. In the off-design simulations, the static pressures and temperatures are calculated based on these values from this table as well.

From Table 6 the high pressure turbine pressure ratio of the calculated cycle is approximately 2.7 and the low pressure turbine pressure ratio is approximately 2.2. A higher compressor pressure ratio can be achieved, which will allow the turbofan engine to run with higher overall efficiency.

Lastly, from the data that was analyzed the enthalpy-entropy diagram (H-S diagram), the temperature-entropy diagram (T-S diagram) and the pressure-volume diagram (P-V diagram) was generated. Figure 18 is the enthalpy-entropy diagram (H-S diagram) of the calculated cycle is displayed. Figure 19 is the temperature-entropy diagram (T-S diagram) of the calculated cycle is displayed. Figure 20 is the pressure-volume diagram (P-V diagram) of the calculated cycle is displayed. These graphs show how the 2 spool mixed turbofan engine with an afterburner thermodynamic properties changes at different enthalpies, temperatures, and pressures throughout the engine cycles.
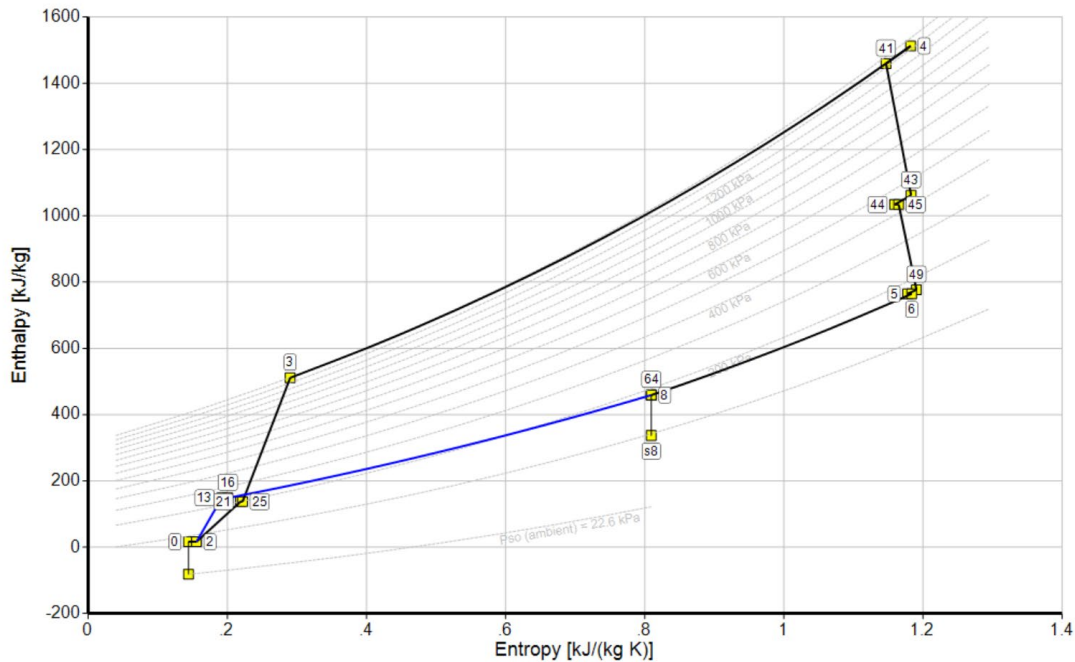
Figure 18. The enthalpy-entropy diagram (H-S diagram)

Figure 19. The temperature-entropy diagram (T-S diagram)

Figure 20. The pressure-volume diagram (P-V diagram)

In this section it was demonstrated how to calculate a turbofan engine cycle and also was able to use the GasTurb the iteration functions. The concepts from this section will be used to analyze the properties for the compressor, combustor and turbine for a turbofan engine with an afterburner.

6.3 The Performance Design Parametric Studies

This section of the chapter will go over performance design parametric studies using the GasTurb software. This section will have one turbofan engine design and the parameters from the turbofan engine will help visualize the different influences that the parameters has on the performance using different diagrams. Once the diagrams are created; the diagrams will be customized by adding contours as well as parameter limits. With these tools, GasTurb enables the user to answer a wide variety of turbofan engine design questions and discover interesting relationships between design and performance parameters.

As mentioned before, the 2 spool mixed turbofan engine with an afterburner configuration will be used. For this part, all of the input data from Table 6 above will be used to conduct a design point simulation as a reference point for the parametric study. The calculated cycle is set at flight conditions of 11,000 Meters altitude and a Mach number of 1.5. The overall pressure ratio (P3/P2) is rather low at 17.33, the burner exit temperature (Station 4) is 1,600K and the bypass ratio (BPR) is 1. This cycle is typical for a small turbofan engine with afterburners.

When setting up the turbofan design point; the compressor pressure ratio and the burner exit temperature parameters were the driving parameters. With parametric studies, one can examine and visualize the influence of one or two parameters on the turbofan cycle. In the parametric study GasTurb can conduct several design point calculations, all with the same input data, but altering the selected parameters whose influence that was examined. The high pressure compressor pressure ratio was the only parameter for the first study. The interval and the step size of the variation of the pressure ratio was defined as a start value of 5, a number of 5 values and a step size of 1. From those values the parametric study began.

The results of the parametric study are presented graphically as shown in Figure 21. The Specific Fuel Consumption was assigned to the y-axis and the Overall Pressure Ratio was assigned to the x-axis.
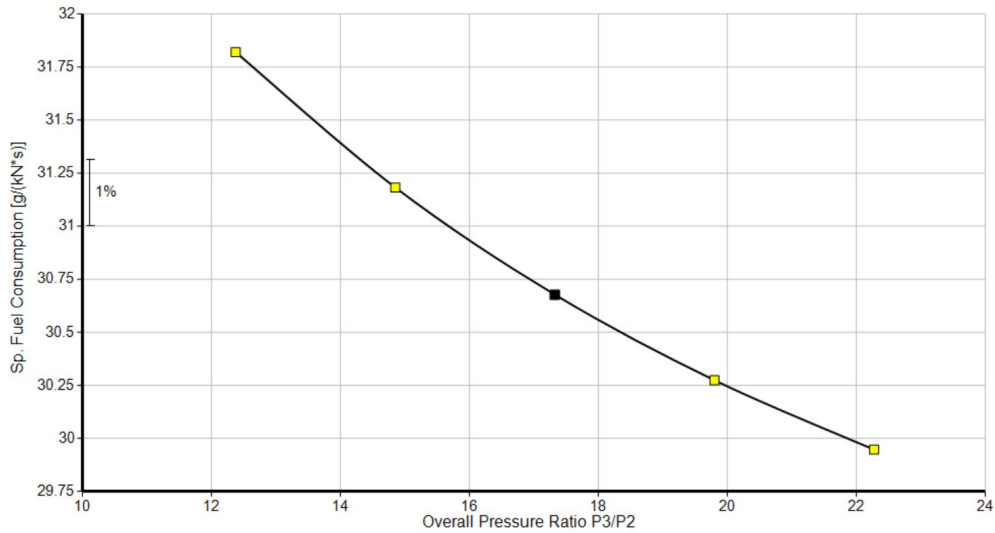
Figure 21. Specific fuel consumption over the overall pressure ratio graph

The results of the parametric study are displayed for the assigned axis-parameters. Each yellow square marks a design point calculation conducted for a different high pressure compressor pressure ratio between 5 and 9. The initial design point calculation is marked with a black square. The graph shows that with a higher overall pressure ratio the specific fuel consumption can be reduced.

Up to 4 y-axes were selected in Figure 22. The high and low pressure turbine pressure ratio as well as the low pressure turbine exit temperature T5 to the y-axis's fields. Figure 22 shows the graph with the 4 ordinate-Parameters.
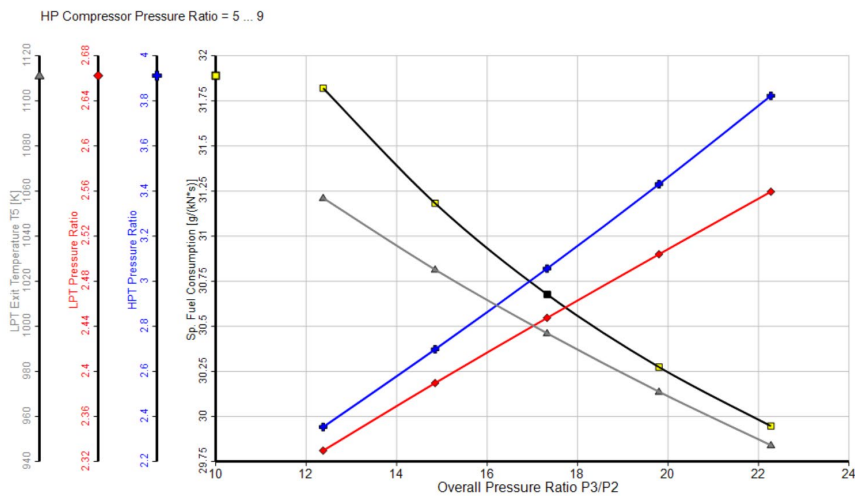
Figure 22. Graph with 4 ordinate-parameters

36

The curves are differentiated by the color as well as the symbols of the plotted points which are displayed on top of each axis. It is shown that when the overall pressure ratio increases, the pressure ratio of both turbines increases as well. Therefore, as the burner exit temperature T4 is not varied. Therefore, the exit temperature of the lower pressure turbine decreases.

Now, another parametric study will be started, in which we will vary the burner exit temperature T4 as well. For the second parameter to be studied is the burner exit temperature. The defined values for the study is 1,600 Kelvin with a step size of 25 Kelvin. Figure 23 below shows the specific fuel consumption over net thrust graph.
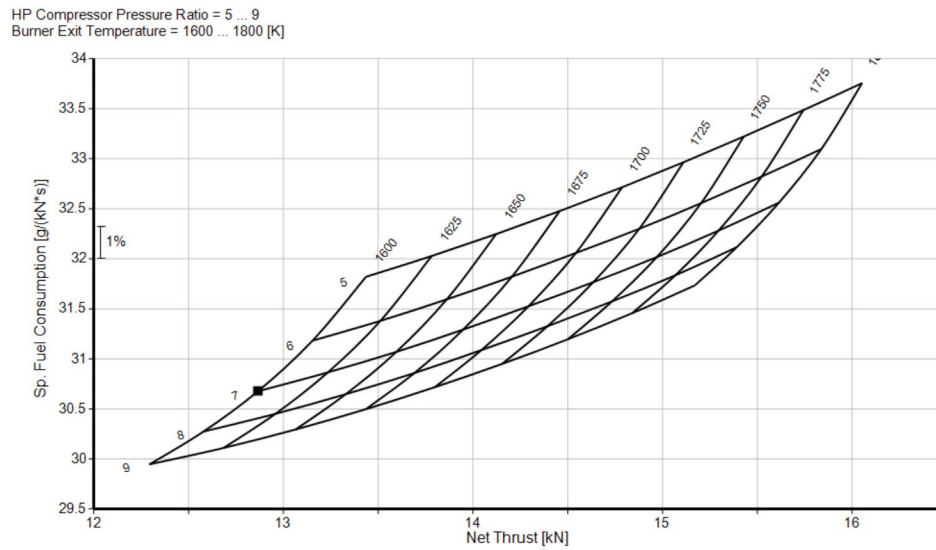
Figure 23. The specific fuel consumption over net thrust graph

For each combination of the varied parameters, a design point calculation was conducted. Isolines connect the design points calculated for the same input parameter value. Thus, the intersection points of the isolines represent the calculated design points. Lastly, the black square marks the initial design point calculation.

To plot a third parameter, a contour plot was used. For this part the core efficiency parameter was examined. As shown in Figure 24 the colored efficiency contour lines are now added to the diagram.
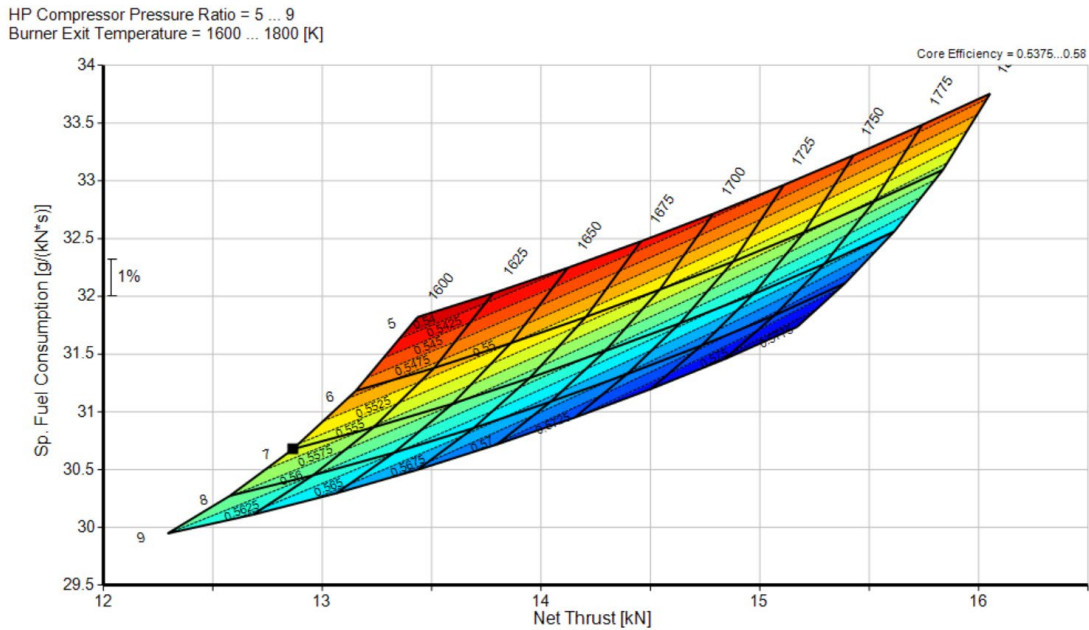
Figure 24. Colored efficiency contour lines added to the graph

As shown in Figure 24 the contour parameter is indicated on the top right corner of the graph. When choosing a turbofan cycle design parameter, many different limits must be kept in mind. To take such limits into account when conducting a parametric study, they can be visualized by using a diagram. In this case the inlet temperature of the LP turbine we will be defined as a limiting factor. This could be due to the turbine material. The LP turbine inlet temperature was selected as a limiting parameter. The value of 1,200 Kelvin was added, which was defined as an upper limit of the graph. Figure 25 below shows a graph with a grey colored. The grey colored area marks the value range that exceeds the limit that was defined. In addition to that, the limited parameter is displayed on the top right corner of the graph.
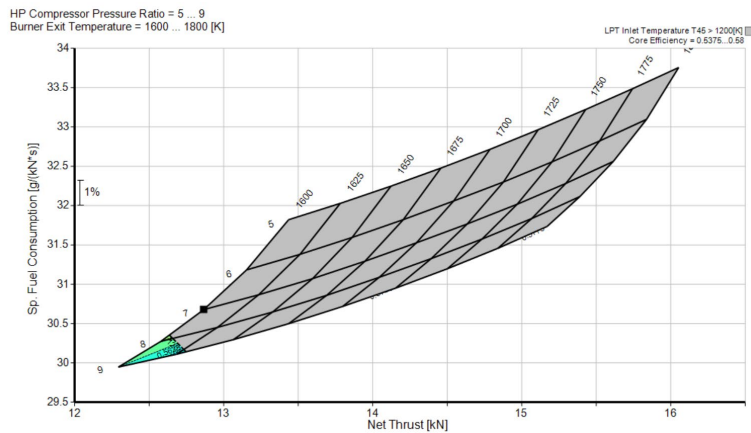
Figure 25. Grey colored specific fuel consumption over net thrust graph

Another graph will be created however, this time the graph will be of the specific fuel consumption over the mixer velocity ratio as shown in Figure 26 below.
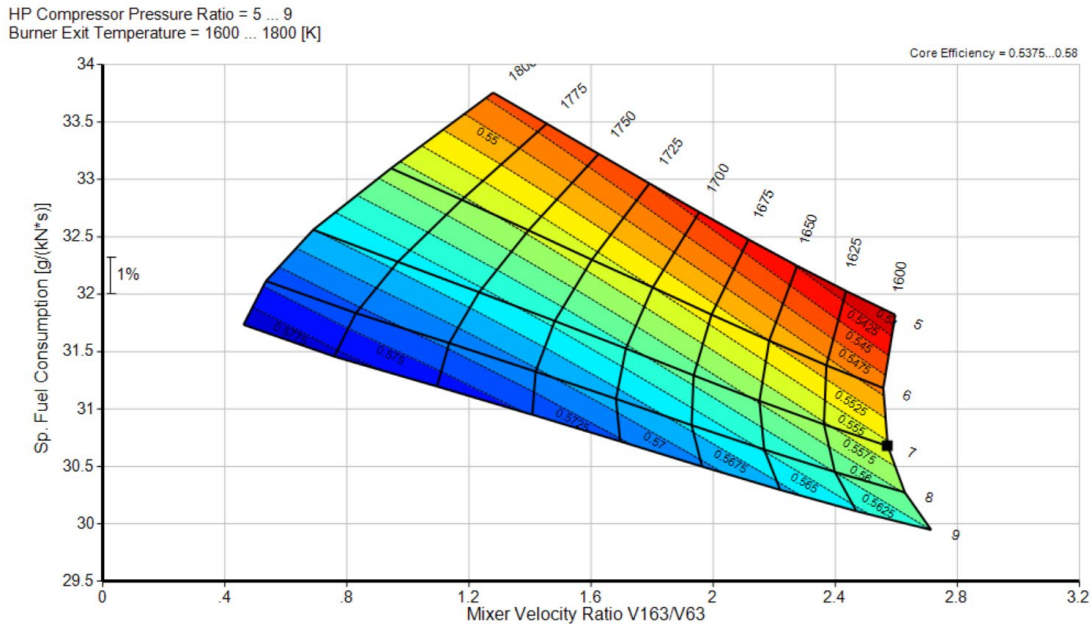
Figure 26. The specific fuel consumption over the mixer velocity ratio graph

The mixer velocity ratio is the relation between the ideal bypass nozzle velocity and the ideal core nozzle velocity, which each are calculated from an isentropic expansion to ambient pressure. As the shown in the graph above, for a optimal design of a 2 spool mixed turbofan engine with an afterburner, the mixer velocity ratio reaches a fixed value related to the LP turbine and the fan efficiencies of the turbofan engine. The turbofan velocity ratio can be influenced via the outer fan pressure ratio. Therefore, all of the cycles are optimized for a low specific fuel consumption.

In this section it was demonstrated how the GasTurb software uses parametric study to simplify the engine design process and to help us discover relationships between design variables and performance results. The concepts from this section will be used to analyze the properties for the compressor, combustor and turbine for a turbofan engine with an afterburner.

6.4 The Off-Design Simulations for a 2 Spool Mixed Turbofan Engine with an Afterburner

This final section of the chapter will go over how the off-design simulations will be performed. To start things off, calculating a single off-design point of a turbofan engine will be done first. The next step will be to examine how GasTurb uses component maps to calculate the

off-design behavior. The last step will be to calculate the turbofan engine operating line. The study will continue to use the 2 spool mixed turbofan engine with an afterburner. First we'll look at the low pressure compressor map and the high pressure compressor map of the turbofan engine that was generated. Figure 27 and Figure 28 shows the low and high pressure compressor graphs, which shows the compressors efficiency and relative spools speeds as a function of the mass flow and pressure ratio.
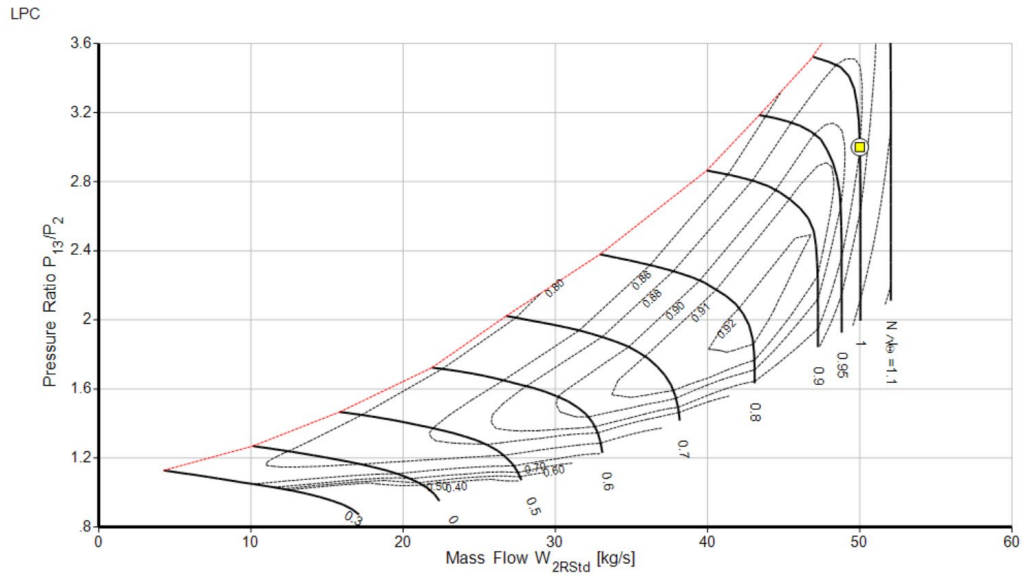
Figure 27. The low pressure compressor graph
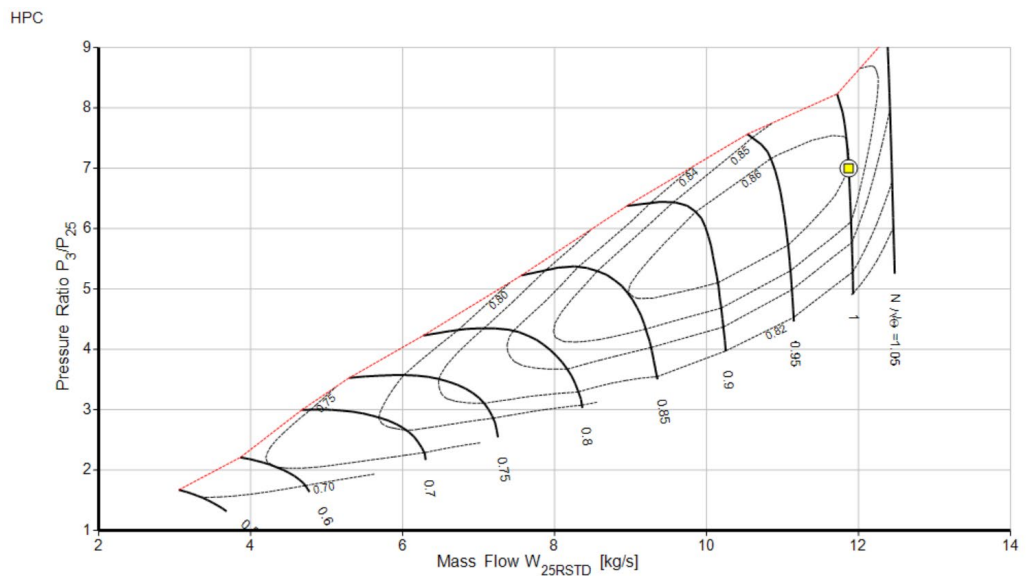
Figure 28. The high pressure compressor graph

In both figures the cycle design point is marked with a circle whilst the yellow square marks the calculated off-design operating point. As the two figures shows, the calculated design point of this off-design point are almost identical. This is due to the fact that, the GasTurb software has already calculated the off-design input for the cycle design point of the turbofan engine. In Figure 28 above the low pressure compressor ratio is 3, with a design compressor efficiency of 88% and a reduced mass flow of 50 kilogram per second. Also, in Figure 28 above is the high pressure compressor ratio is 7, with a design compressor efficiency of 86% and a reduced mass flow of 12 kilogram per second. This shows that the low and high pressure compressor maps are close in value.

The turbine map was examined next. Similar to the compressor, the turbine has a high and low turbine ratios as shown below in Figure 29 and Figure 30.
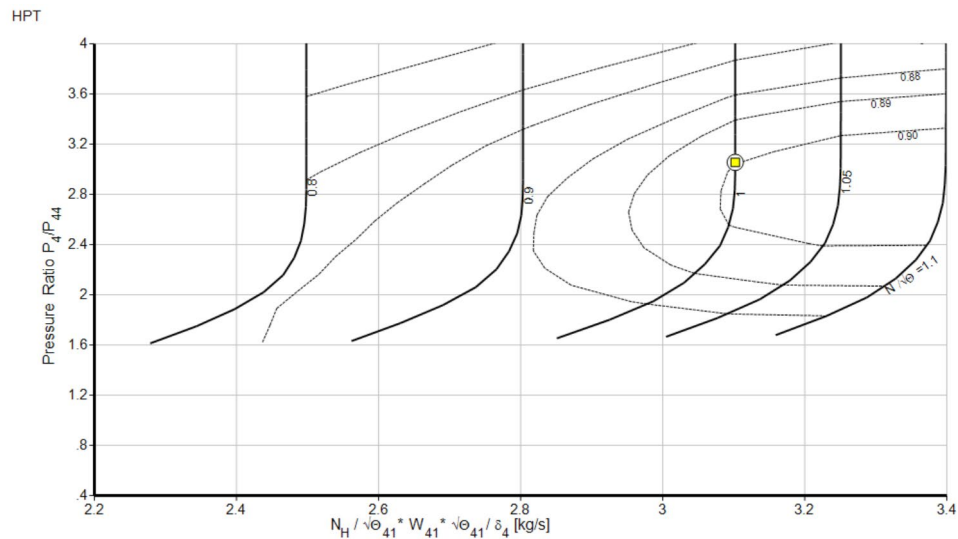
Figure 29. The high turbine ratios graph
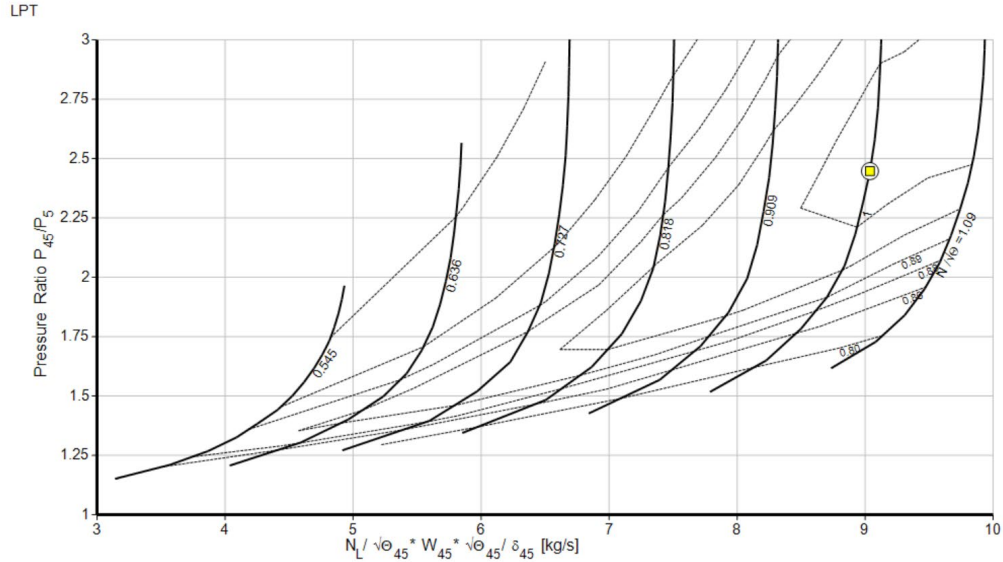
Figure 30. The low turbine ratios graph

The two figures show the graphs turbine efficiencies and relative spool speeds as a function of the turbine pressure ratio and the product of corrected flow and corrected speed. The presentation of the design point and the off-design point is the same as in the compressor map. For the turbine map(s), GasTurb allows one to switch to different graph formats throughout the design process. For example, the axis-assignment of the turbine graph can be selected and changed. Either the pressure ratio or the corrected work can be selected for the y-axis. The x-axis may be displayed as either the product of the corrected flow and corrected speed or corrected speed or corrected flow. In this case the turbine pressure ratio is shown versus the product of corrected flow and corrected speed. Figure 31 and Figure 32 is the high and low turbine pressure ratio versus the product of corrected flow and corrected speed. Figure 31 shows the high turbine pressure ratio with the corrected speed as the x-axis value. The corrected flow is shown as contour lines in the percentage of the maximum corrected flow in the graph. Also, Figure 32 shows the low turbine pressure ratio with the corrected speed as the x-axis value. Just as the high turbine pressure ratio the low turbine pressure ratio corrected flow is shown as contour lines in the percentage of the maximum corrected flow on the graph.
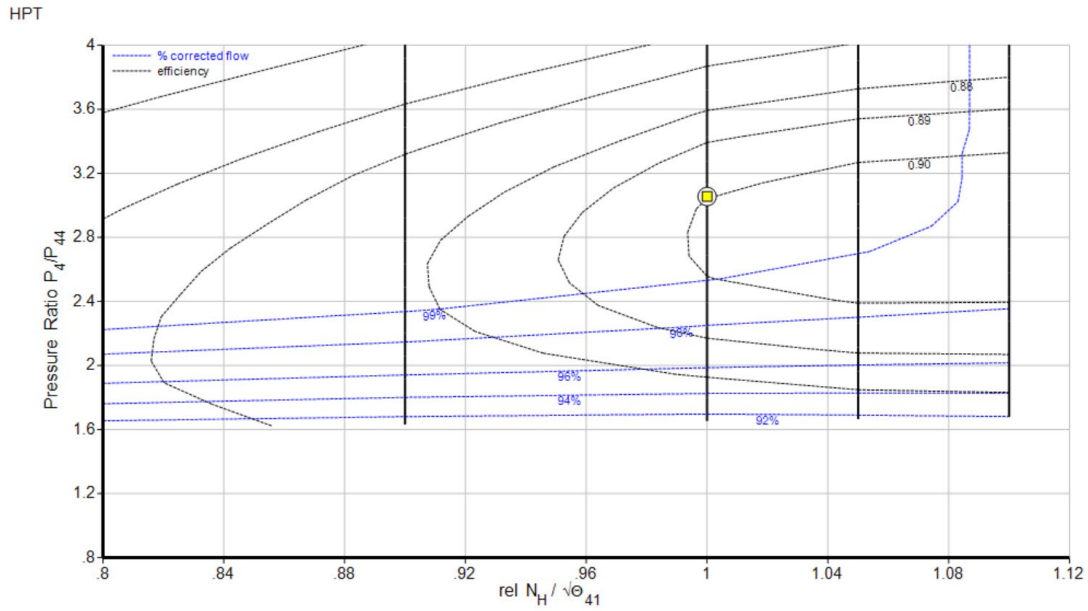
Figure 31. The high turbine pressure ratio versus the corrected flow/corrected speed graph
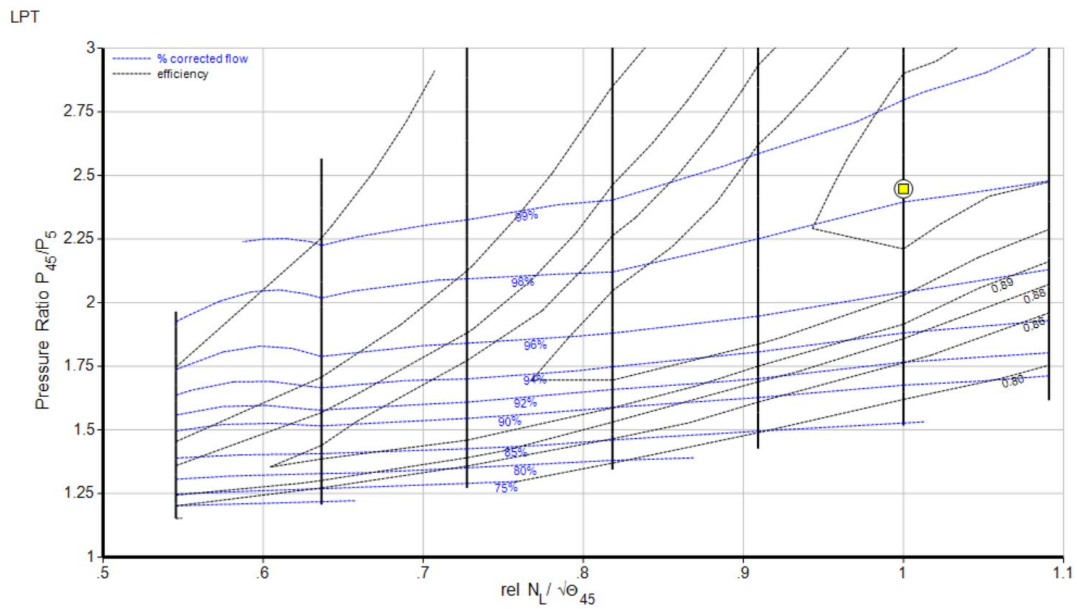
Figure 32. The low turbine pressure ratio versus the corrected flow/corrected speed graph

When choosing the corrected mass flow as the x-axis value, as is standard for the compressor, the readability of the graph can be poor if the speed lines collapse in the region of choked flow. Figure 33 shows the high pressure turbine and Figure 34 shows the low pressure turbine.

HPT
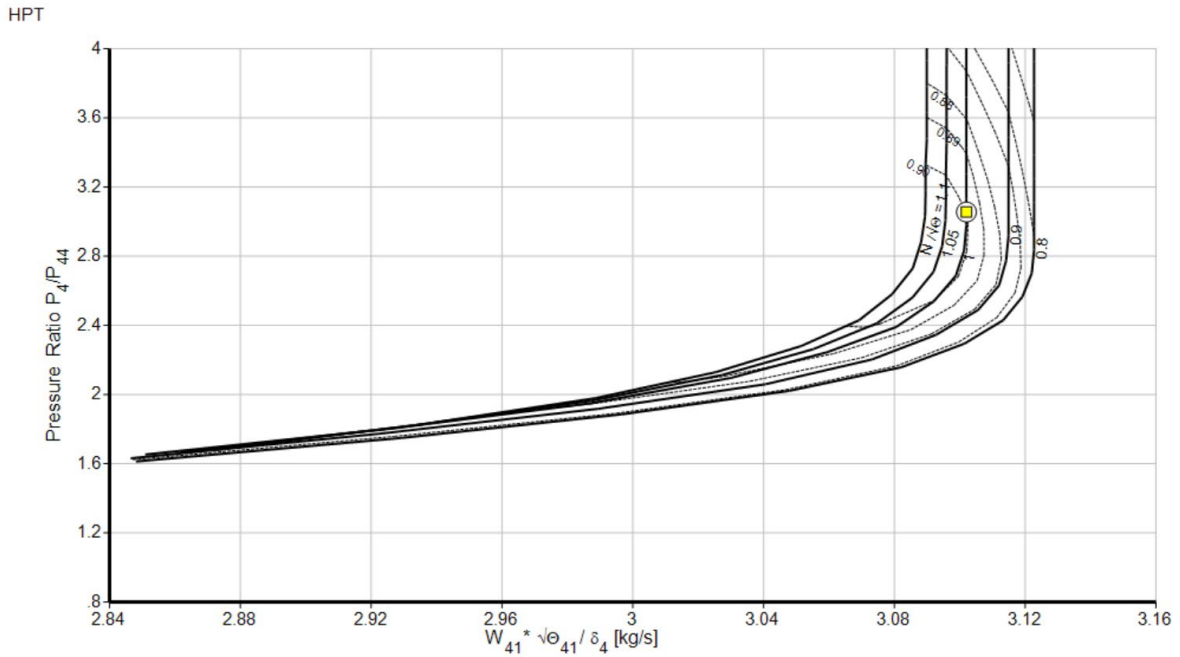
Figure 33. The high pressure turbine graph

LPT
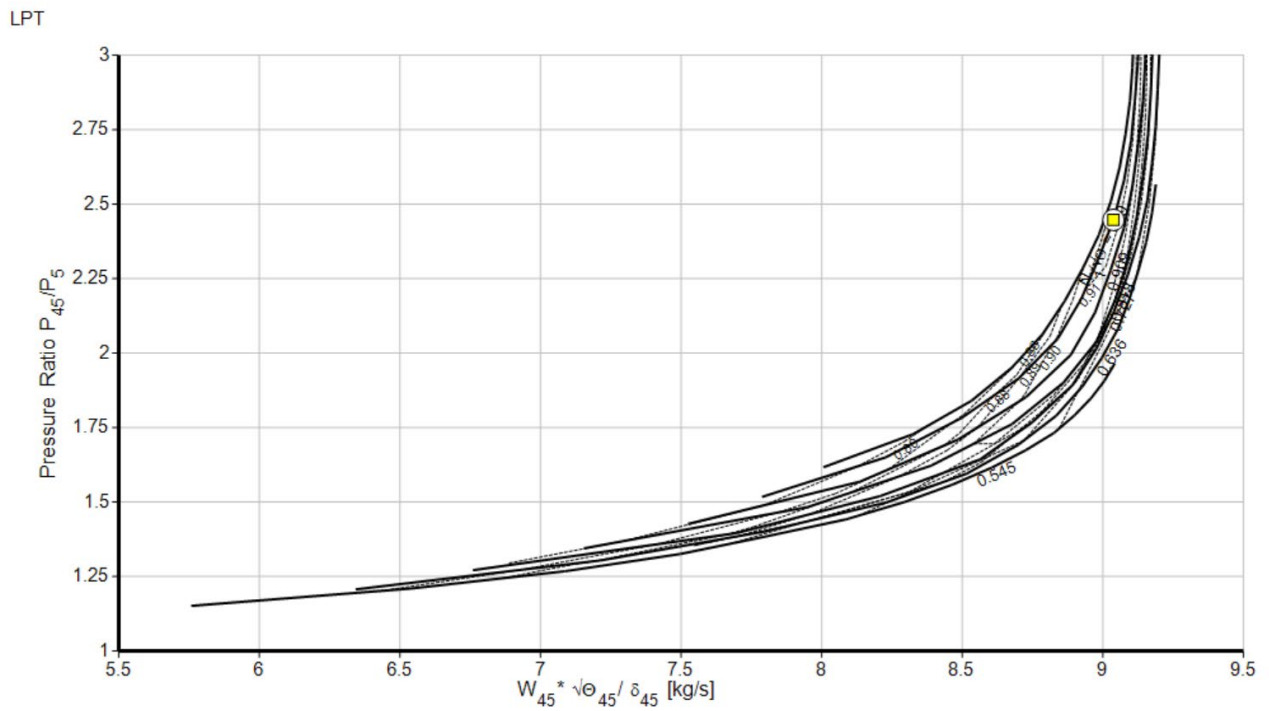
Figure 34. The low pressure turbine graph

44

Figure 33 and Figure 34 show that the high and low pressure turbine graphs are close in value.

Next, we'll look at Table 7 below to get the details at the thermodynamic stations. Table 7 is the stations data of the turbofan engine. In off-design simulations, the static pressures and temperatures are calculated using the flow areas calculated at the design point. The engine geometry is fixed during the design point calculation as shown in Figure 35 below.

Table 7. The thermodynamic stations data for the turbofan engine

	Units	St 2	St 21	St 25	St 3	St 4	St 44	St 45	St 5	St 6	St 13	St 16	St 64	St 8
Mass Flow	kg/s	37.7409	18.8704	18.8705	18.3043	16.7176	18.6047	18.6047	19.1708	19.1708	18.8704	18.8704	38.0412	38.0412
Total Temperature	K	314.282	433.978	433.978	788.356	1600	1220.48	1220.48	996.888	996.888	444.876	444.876	735.268	735.268
Static Temperature	K	299.368	413.71	413.71	782.752	1579.25	1183.48	1191.12	957.843	989.306	431.366	438.155	727.444	622.748
Total Pressure	kPa	79.8747	199.687	197.69	1383.83	1342.32	439.212	430.428	175.868	172.351	239.624	232.435	181.219	181.219
Static Pressure	kPa	67.3404	168.452	166.767	1346.96	1266.96	385.426	388.105	149.501	167.084	214.732	220.185	173.922	96.7337
Velocity	m/s	173.421	203.438	203.438	110.374	229.618	300.264	267.716	301.949	133.052	166.096	117.154	131.384	494.288
Area	m²	0.277714	0.065393	0.066053	0.027664	0.02605	0.054612	0.061222	0.116764	0.244889	0.065513	0.092007	0.347626	0.142221
Mach Number		0.500001	0.5	0.500001	0.200002	0.3	0.450002	0.400002	0.499999	0.217001	0.400001	0.28	0.247004	1
Density	kg/m³	0.783633	1.41847	1.40429	5.99476	2.79485	1.13457	1.13512	0.543748	0.588371	1.73418	1.75066	0.832915	0.541141
Spec Heat @ T	J/(kg*K)	1006.04	1018.94	1018.94	1095.93	1275.87	1220.75	1220.75	1177.93	1177.93	1020.68	1020.68	1099.16	1099.16
Spec Heat @ Ts	J/(kg*K)	1004.78	1015.69	1015.69	1094.59	1273.57	1214.63	1215.98	1169.25	1176.25	1018.52	1019.6	1097.21	1070.96
Enthalpy @ T	J/kg	16259.4	137396	137396	511117	1.51274E6	1.03394E6	1.03394E6	764661	764661	148523	148523	459023	459023
Enthalpy @ Ts	J/kg	1221.97	116703	116703	505026	1.48637E6	988866	998109	719074	755809	134729	141660	450393	336863
Entropy Function @ T		0.184948	1.32185	1.32185	3.50627	6.58122	5.38416	5.38416	4.53402	4.53402	1.41006	1.41006	3.28099	3.28099
Entropy Function @ Ts		0.01425	1.15175	1.15175	3.47926	6.52345	5.25353	5.28066	4.37159	4.50298	1.30038	1.35591	3.23989	2.65324
Exergy	J/kg	95540.8	202958	202333	561221	1.36976E6	895933	894677	622599	621343	219938	218043	396731	396731
Gas Constant	J/(kg*K)	287.05	287.05	287.05	287.05	287.046	287.047	287.047	287.047	287.047	287.05	287.05	287.049	287.049
Fuel-Air-Ratio		0	0	0	0	0.024179	0.021674	0.021674	0.02102	0.02102	0	0	0.010484	0.010484
Water-Air-Ratio		0	0	0	0	0	0	0	0	0	0	0	0	0
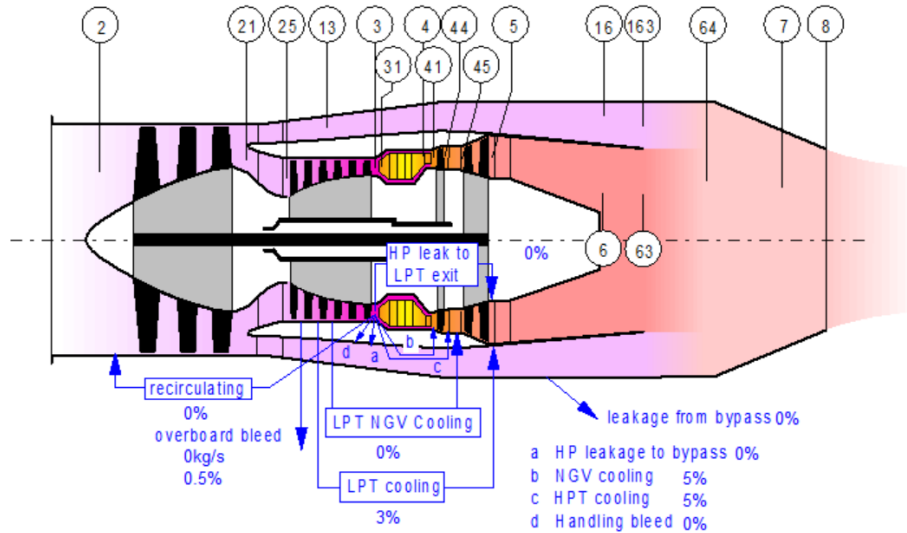
Figure 35. The 2 spool mixed turbofan engine with an afterburner labelled with sae notation

Afterwards the next step that was done was to examine an off-design point and vary the burner exit temperature. GasTurb allows the user to change the relative spool speed or the burner exit temperature. Therefore, it was decided to switch to the burner exit temperature option and reduce the burner exit temperature to 1,200 Kelvin for the next off-design calculation. The predetermined burner exit temperature is given in Table 8 below.

Table 8. Off-design calculation data

```
           W         T         P      WRstd
Station   kg/s       K        kPa     kg/s        FN        =      4.98 kN
amb               216.65    22.632
  1      26.126    314.28    83.127               TSFC      =     31.1038 g/(kN*s)
  2      26.126    314.28    79.875   34.612      WF Burner=      0.15479 kg/s
 13      14.394    392.82   160.610   10.603      s NOX     =      0.2576
 21      11.732    384.46   140.426    9.778      BPR       =      1.2269
 25      11.732    384.46   139.454    9.846      Core Eff  =      0.4788
  3      11.380    647.44   740.856    2.333      Prop Eff  =      0.8247
 31      10.148    647.44   740.856               P3/P2     =      9.275
  4      10.303   1200.00   716.242    2.974      P5/P2     =      1.2646 EPR
 41      10.889   1172.04   716.242    3.107      P16/P6    =      1.56268
 43      10.889    921.68   233.749               A63       =      0.30047 m²
 44      11.476    908.41   233.749               A163      =      0.04715 m²
 45      11.476    908.41   229.075    9.013      A64       =      0.34763 m²
 49      11.476    756.00   101.006               XM63      =      0.16216
  5      11.828    749.94   101.006   19.141      XM163     =      0.83992
  6      11.828    749.94    99.252               XM64      =      0.24634
 16      14.394    392.82   155.099               P63/P6    =      0.99137
 64      26.222    558.61   108.288               P163/P16  =      0.98846
  8      26.222    558.61   108.288   34.162      A8        =      0.14971 m²
Bleed    0.059     647.44   740.852               CD8       =      0.95000
-----------------------------------------        Ang8      =        25.00 °
Efficiencies:   isentr  polytr   RNI    P/P       P8/Pamb   =      4.78473
  Outer LPC     0.8807  0.8917  0.711  2.011      WLkBy/W25=      0.00000
  Inner LPC     0.7806  0.7972  0.711  1.758      WCHN/W25  =      0.05000
  HP Compressor 0.8641  0.8909  0.976  5.313      WCHR/W25  =      0.05000
  Burner        0.9970                 0.967      Loading   =      306.20 %
  HP Turbine    0.8922  0.8780  1.364  3.064      WCLN/W25  =      0.00000
  LP Turbine    0.8906  0.8798  0.585  2.268      WCLR/W25  =      0.03000
  Mixer         0.5000                            WBHD/W21  =      0.00000
-----------------------------------------        far7      =      0.00594
HP Spool mech Eff 1.0000  Speed   19053 rpm       WBLD/W25  =      0.00500
LP Spool mech Eff 1.0000  Speed   10688 rpm       PWX       =        50.0 kW
-----------------------------------------        P16/P13   =      0.9657
P2/P1= 0.9609 P25/P21=0.9931 P45/P44= 0.9800      P6/P5     =      0.9826
```

When comparing Table 4 to Table 2 mentioned earlier, the engine mass flow (W kg/s) and the pressure ratio (P/P) are significantly reduced leading to a lower net thrust (FN). Figure 36 shows the low pressure compressor graph. One can see that the off-design point with the reduced pressure ratio and mass flow is derived for a burner exit temperature of 1,200 Kelvin. In addition to that, Figure 37 shows the high pressure compressor graph. Just like with the low pressure compressor, the high pressure compressor graph has an off-design point with the reduced pressure ratio and mass flow derived for a burner exit temperature of 1,200 Kelvin.
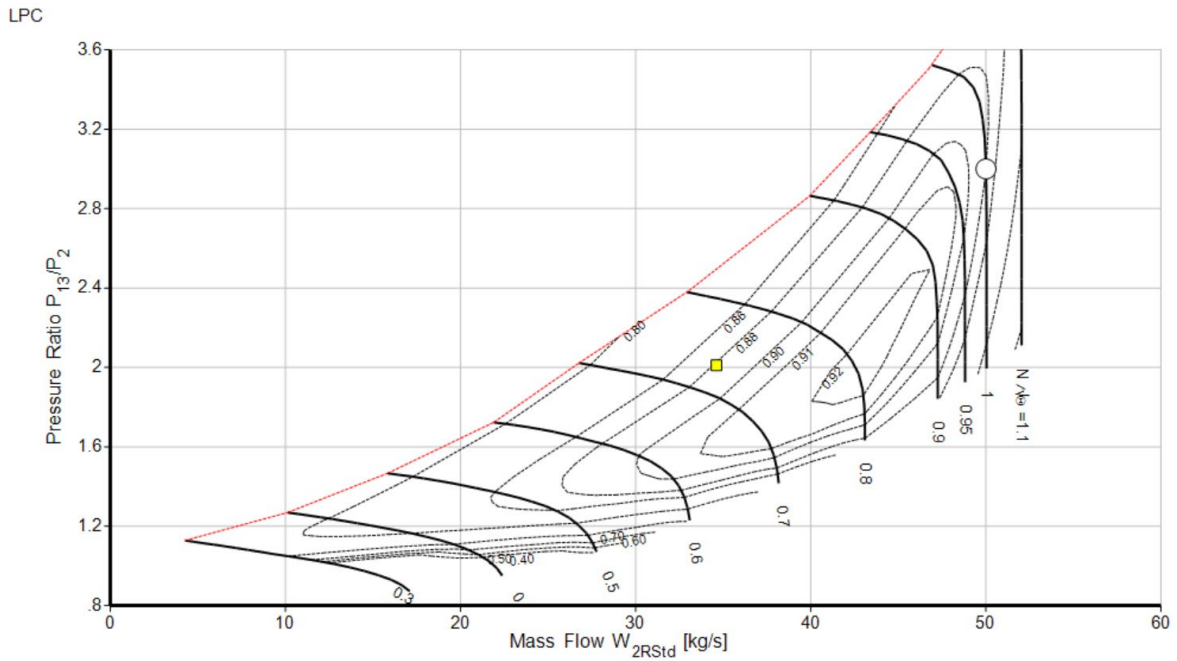
Figure 36. The low pressure compressor graph
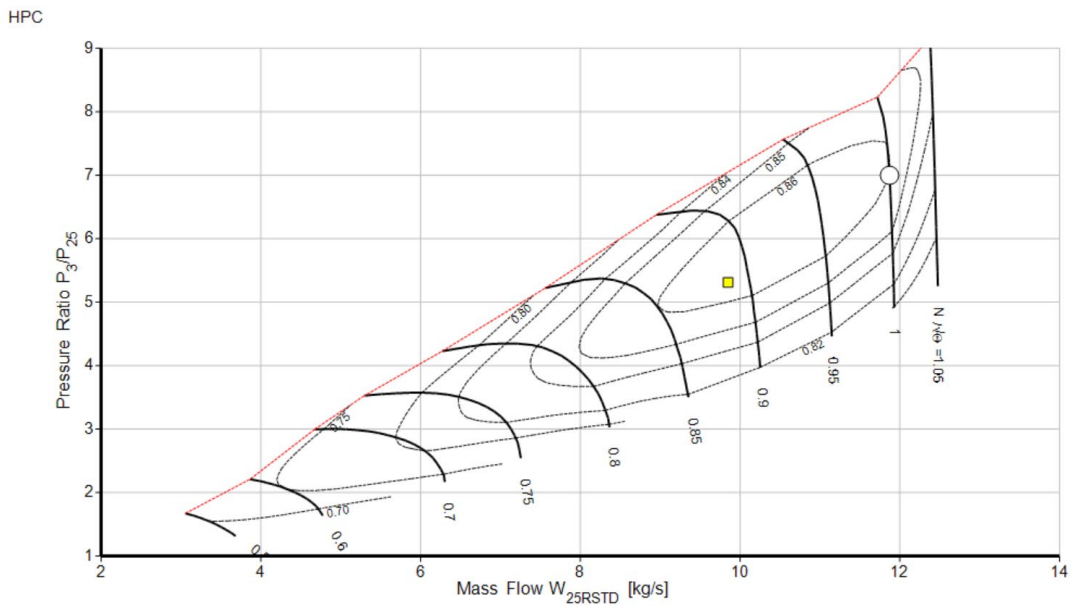
Figure 37. The high pressure compressor graph

Lastly, the operating line for this turbofan engine was calculated. In order to calculated this, the HPC spool speed parameter is set to 1. Afterwards, the operating line commences with the point that was defined. Once this happens a series of points with decreasing spool speed will be calculated. The number of calculated points and the step size can be specified. As shown in Figure 38 the operating line of the low pressure compressor is displayed with 20 points and a step size of 2.5% of the relative spool speed. Just like the low pressure compressor graph, the high pressure compressor graph shown in Figure 39 is displayed with 20 points and a step size of 2.5% of the relative spool speed.
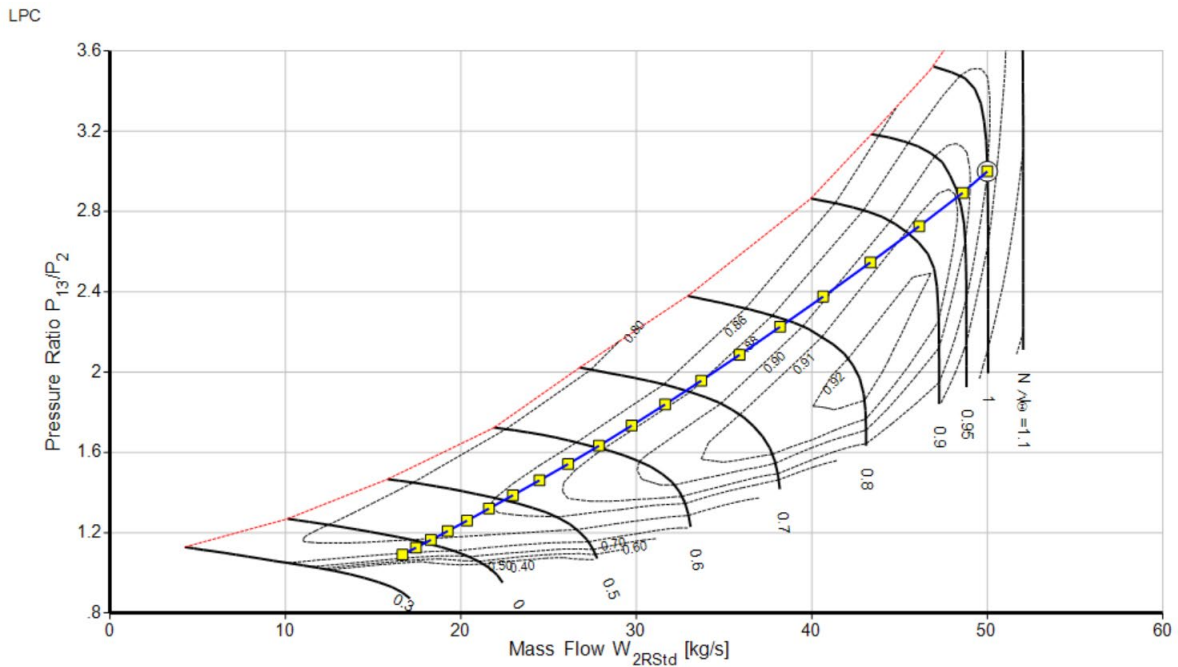
Figure 38. The operating line of the low pressure compressor graph
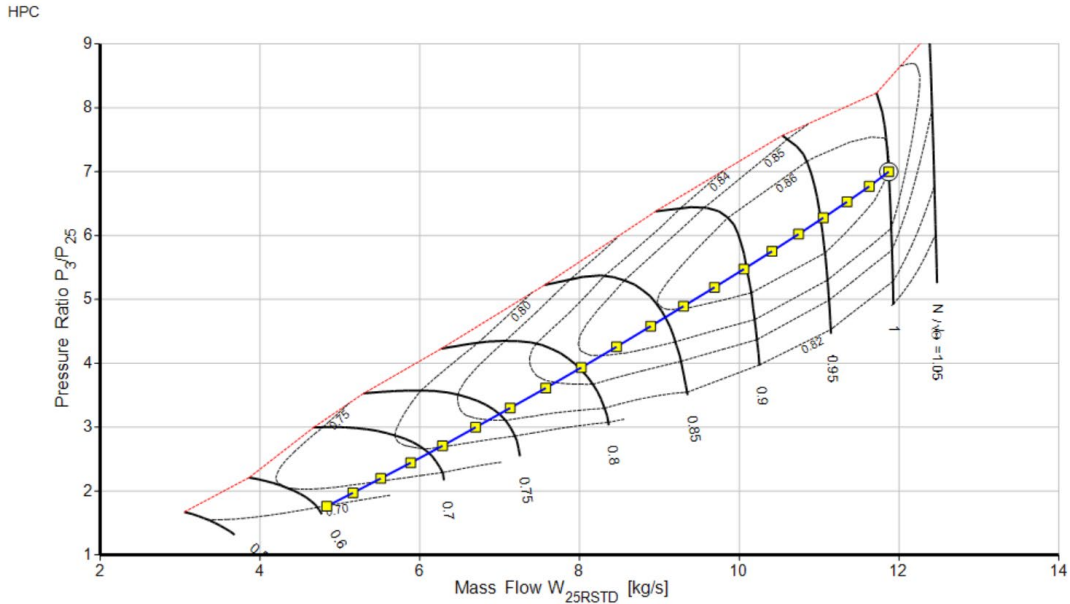
Figure 39. The operating line of the high pressure compressor graph

In this section it was demonstrated how the off-design simulations was done GasTurb software. In addition to that, this chapter demonstrated how to calculate a turbofan engine cycle and also was able to use the GasTurb the iteration functions. Also, how the GasTurb software uses parametric study to simplify the engine design process and to help us discover relationships between design variables and performance results. The next chapter of this report will cover the analysis done using the parametric cycle analysis for real engines. This analysis will be done using MATLAB software. The equations and concepts from this report will be used to design the properties for the compressor, combustor and turbine for a turbofan engine with an afterburner.

Chapter 7 – Performance Analysis of a Turbofan Engine Using MATLAB

7.1 Performance Analysis of a Turbofan Engine Using MATLAB

7.1.1 Methodology

MATLAB was used to solve to model the velocity, temperature at the inlet, the pressure at the inlet, temperature of the fan, pressure of the fan, temperature of the compressor, pressure of the compressor, temperature of the high compressor and pressure of the high compressor. In addition to that, equations were set up using MATLAB for a performance analysis for a turbofan engine. Once these parameters were calculated, the results were then plotted against a range of Mach numbers. To find the results, code was used to calculate various parameters and then used to graph the results over a range of Mach numbers that ranged between Mach 0 to 5 for a ideal turbofan engine. The graphs were all created using MATLAB's built-in plotting functions. This allowed one to view the different graphs easily.

7.1.2 Analysis

Figure 40 shows that when starting the velocity at Mach 0 and increasing to Mach 5, the results showed that the velocity reached 19.6 m/s in a linear fashion. Figure 41 shows that when starting the velocity at Mach 0 and increasing to Mach 5, the results showed that the temperature at the inlet reached 2150K in an increasing fashion. Figure 42 shows that when starting the velocity at Mach 0 and increasing to Mach 5, the results showed that the pressure at the inlet reached 6.7×10^2 Pa in an increasing fashion. Figure 43 shows that when starting the velocity at Mach 0 and increasing to Mach 5, the results showed that the temperature of the fan reached 5450K in an increasing fashion. Figure 44 shows that when starting the velocity at Mach 0 and increasing to Mach 5, the results showed that the pressure of the fan reached 2×10^7 Pa in an increasing fashion. Figure 45 shows that when starting the velocity at Mach 0 and increasing to Mach 5, the results showed that the temperature of the compressor reached 13700K in an increasing fashion. Figure 46 shows that when starting the velocity at Mach 0 and increasing to Mach 5, the results showed that the pressure of the compressor reached 14.9×10^7 Pa in an increasing fashion. Figure 47 shows that when starting the velocity at Mach 0 and increasing to Mach 5, the results showed that the temperature of the high compressor reached 1.6×10^4 K in an increasing fashion. Lastly, Figure 48 shows that when starting the velocity at Mach 0 and increasing to Mach 5, the results showed that the pressure of the high compressor reached 2.25×10^8 Pa in an increasing fashion. Furthermore, one can note that for each graph as the Mach number increases so does the graphs.

7.1.3 Results
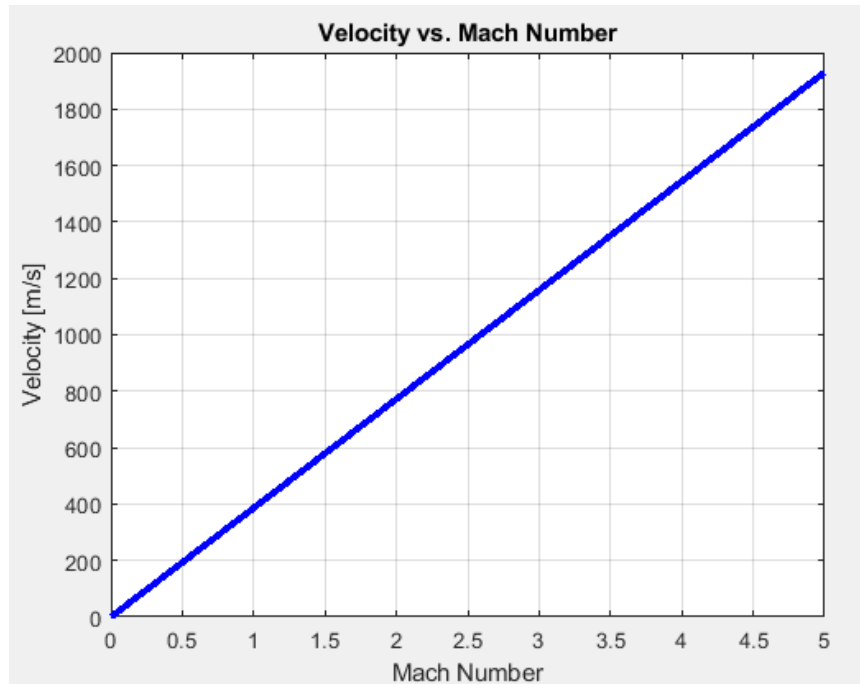
Figure 40. Velocity vs Mach number
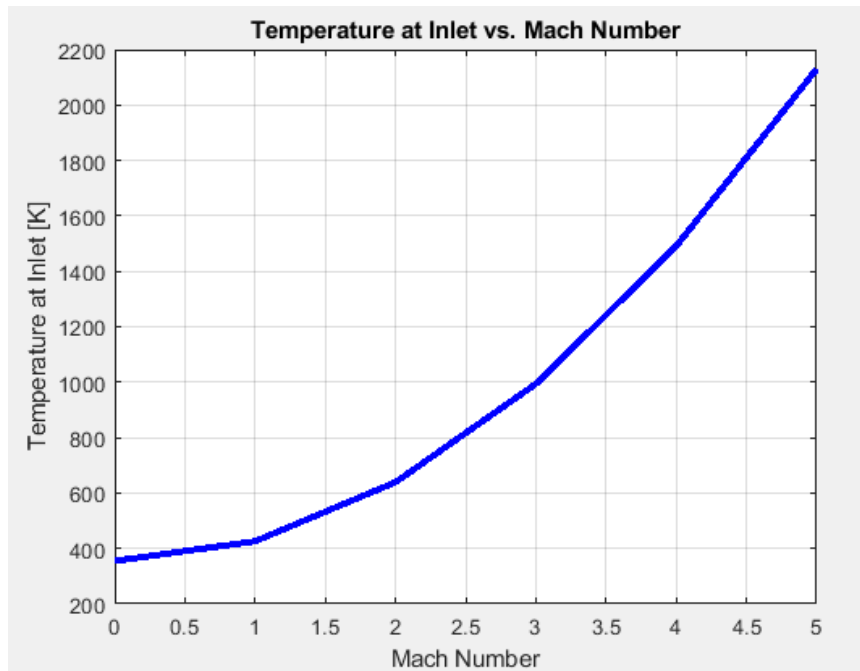
Figure 41. Temperature at the inlet vs Mach number
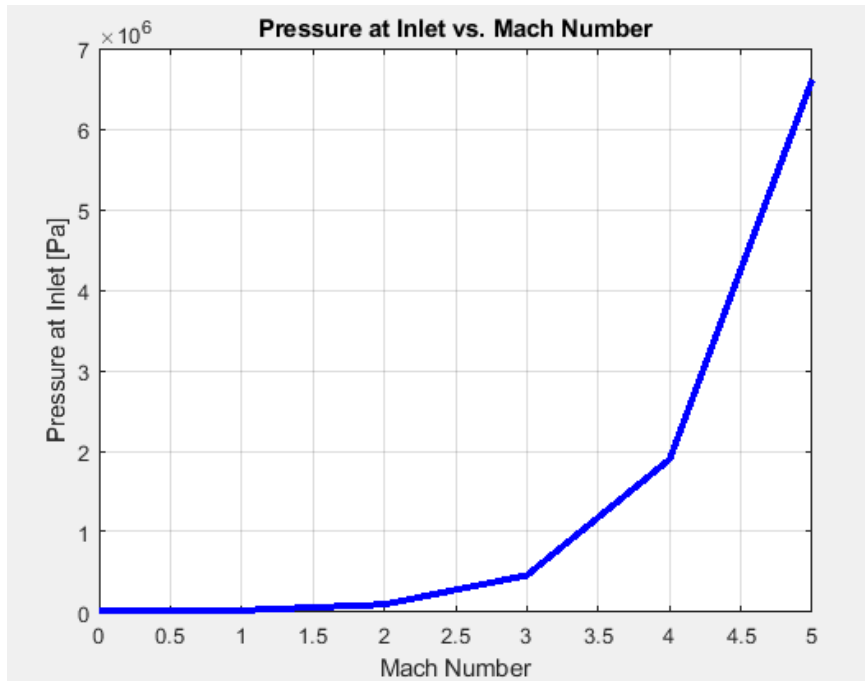
Figure 42. Pressure at the inlet vs Mach number
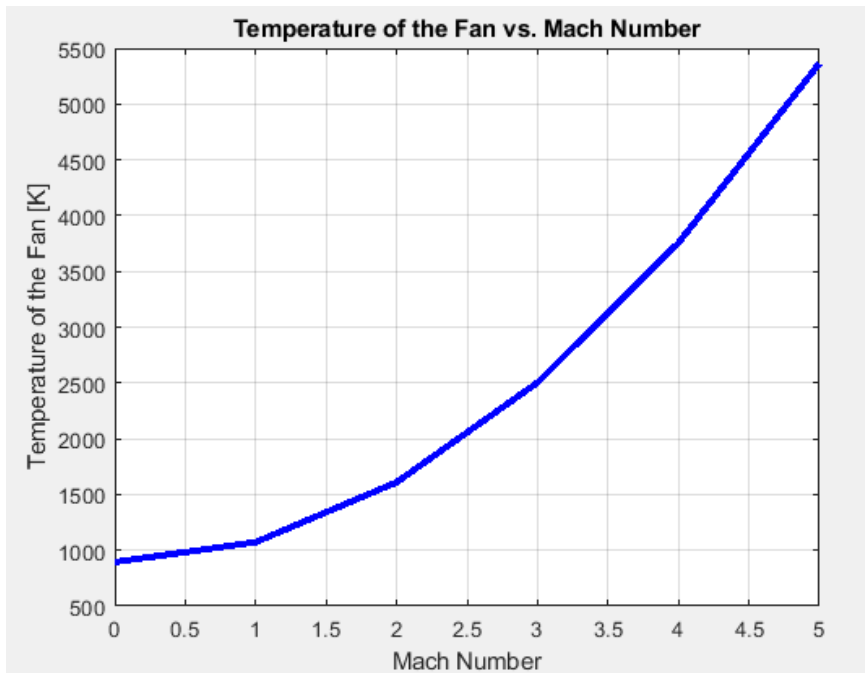
Figure 43. Temperature of the fan vs Mach number
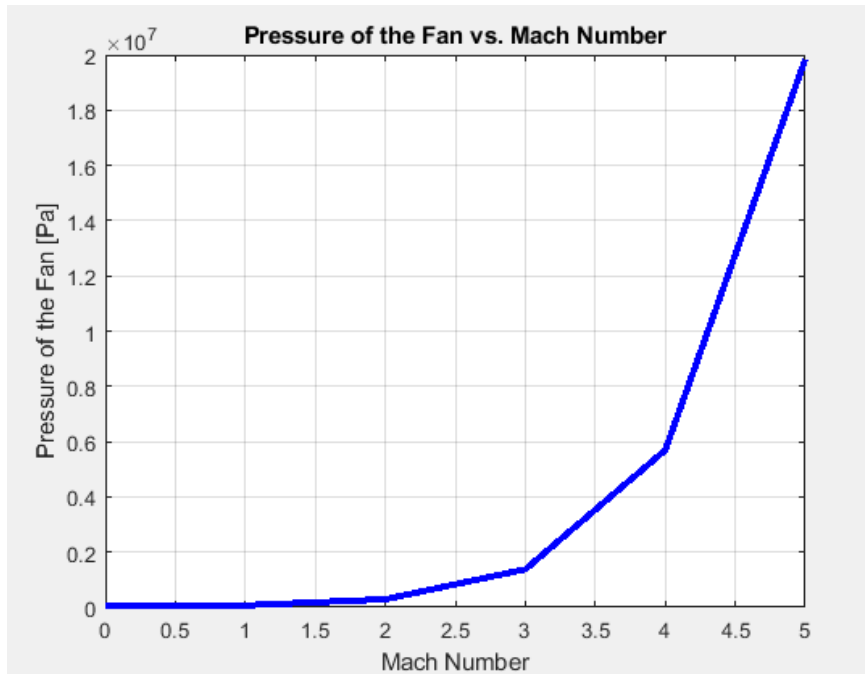
Figure 44. Pressure of the fan vs Mach number
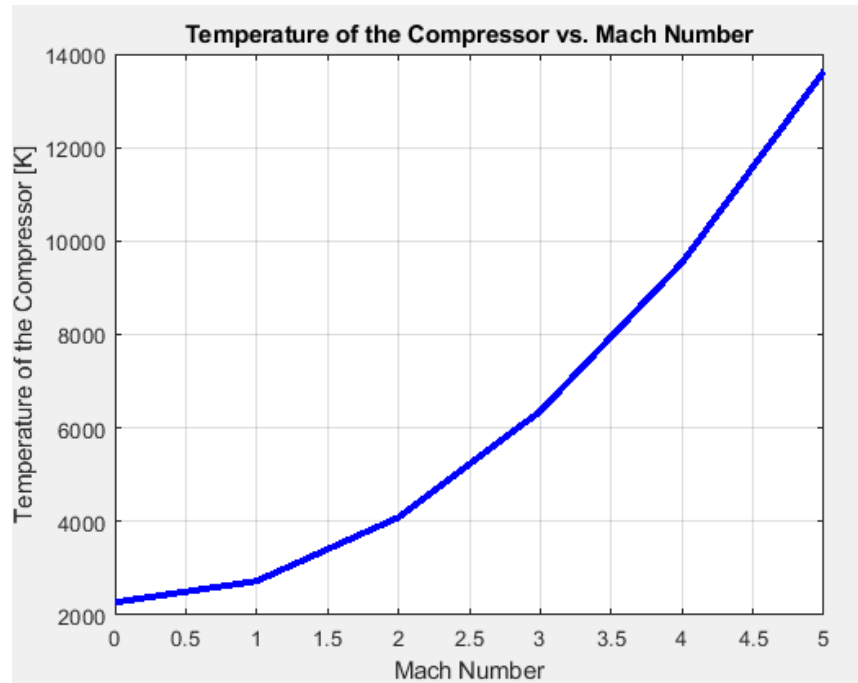
Figure 45. Temperature at the compressor vs Mach number
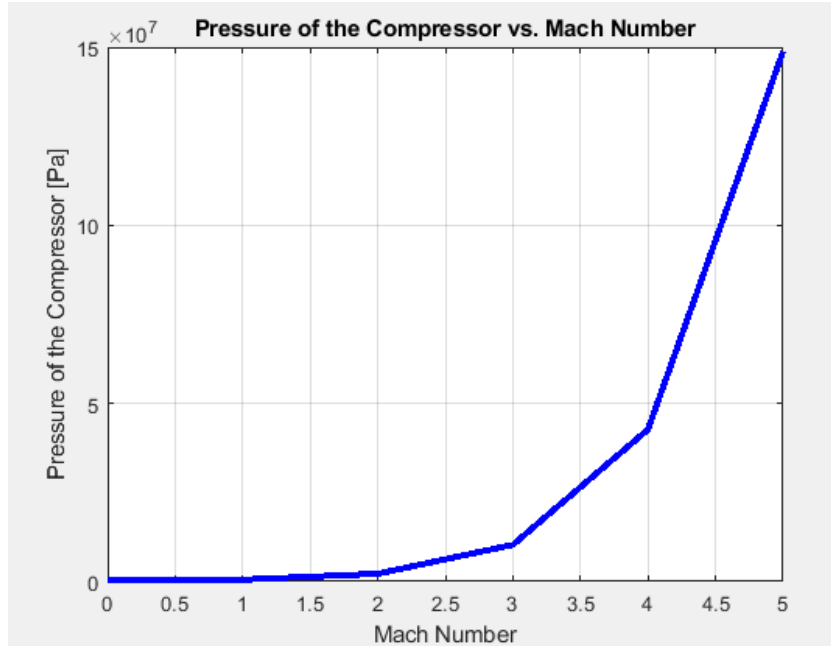
Figure 46. Pressure of the compressor vs Mach number
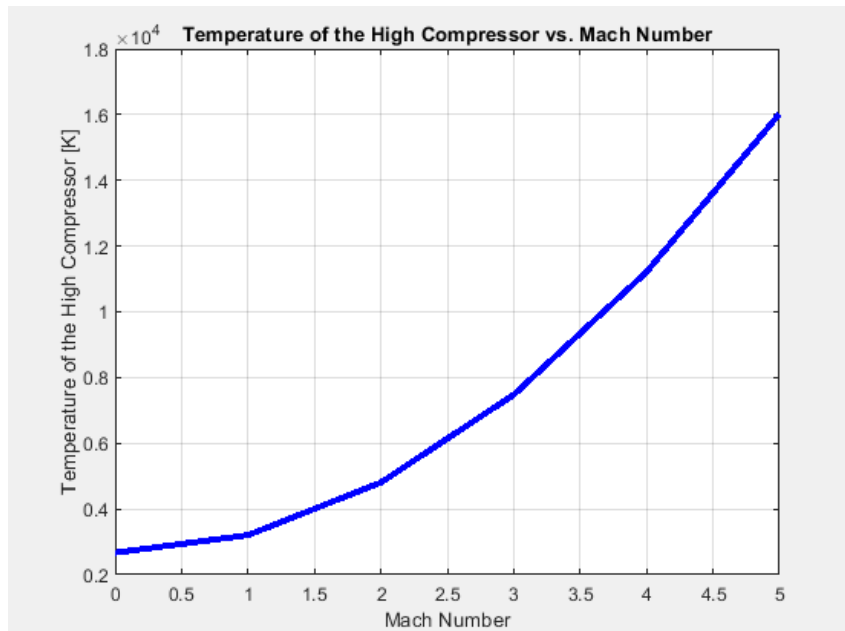
Figure 47. Temperature of the high compressor vs Mach number
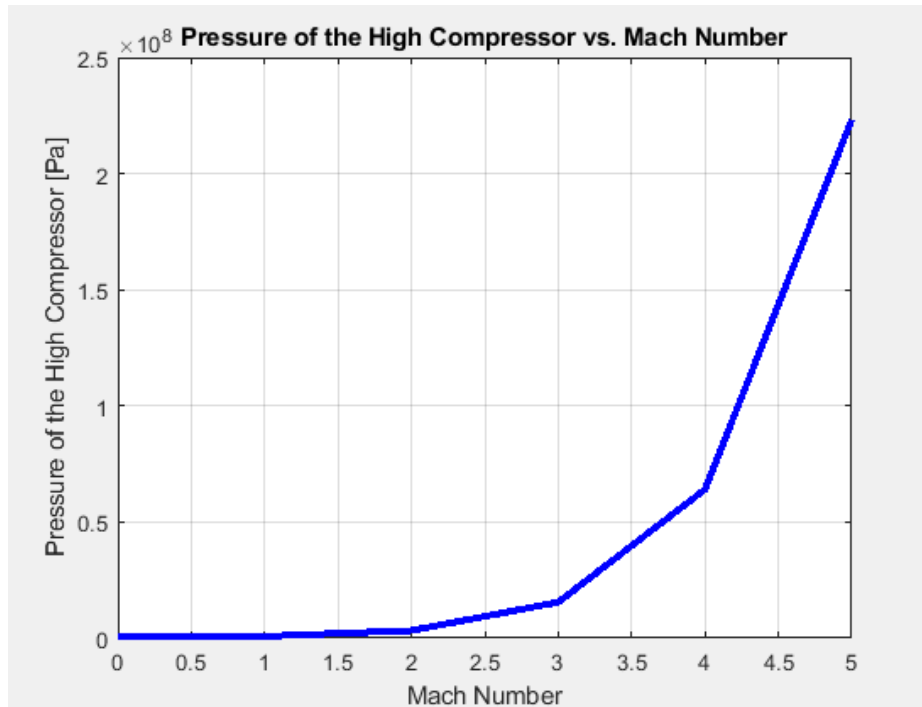
Figure 48. Pressure of the high compressor vs Mach number

In this section the performance analysis of a turbofan engine was demonstrated using MATLAB. In addition to that, MATLAB was successfully able to calculate various parameters and then used to graph the results over a range of Mach numbers that ranged between Mach 0 to 5. The final chapter of this report will be the conclusion of analyses on the Design of a Efficient Turbofan Engine with Afterburner(s).

Chapter 8 – Conclusion

The primary purpose of this study was to design an efficient turbofan engine that included afterburners. The modelling and simulation of the turbofan engine that included afterburners was done using GasTurb and MATLAB software packages. Since this turbofan engine was to include afterburners, it was greatly needed for the engine to be efficient. This meant that the design of the engine from its inlet to the afterburners should be designed efficient to compress the high-speed air that would be flowing through it. Therefore, there were different simulations that was done at different Mach numbers. The Mach numbers were 0 through 5. The trends from the graphs was observed to have contour plots.

Theory states that if the pressure in the combustion chamber is high then there will be a chance for an efficient combustion process. At times there were slight discrepancies in the values calculated however, these discrepancies is possibly a result of an error in the MATLAB code. Nevertheless, this study was just a small step in designing an efficient turbofan engine with an afterburner. Building on this study, future studies can look at the numerous other combinations of mass flow rates of oxygen and other fuels. After the validation of the modelling and simulation of the turbofan engine with an afterburner, different scenarios of the turbofan engine were studied as shown in the graphs.

In the future, new turbofan engine designs will possibly require new propulsion systems. Propulsion capabilities are essential when it comes to increasing the efficiency of the turbofan engine, the durability, mission proficiency, etc. Furthermore, this project has explored a possible future propulsion system design that included an afterburner. For this to be possible, new and improved additive materials could be explored as well as the manufacturing processes and technological advances which would provide solutions to issues. A system like this could be used to replace the traditional turbofan engine propulsion systems.

References

[1] Balli, O., "Exergy modeling for evaluating sustainability level of a high by-pass turbofan engine used on Commercial Aircrafts," Applied Thermal Engineering Volume 123, August 2017, Pages 138-155, *Applied Thermal Engineering* Available: https://www.sciencedirect.com/science/article/abs/pii/S1359431117319269.

[2] Balli, O., "Exergy modeling for evaluating sustainability level of a high by-pass turbofan engine used on Commercial Aircrafts," Applied Thermal Engineering Volume 123, August 2017, Pages 138-155, *Applied Thermal Engineering* Available: https://www.sciencedirect.com/science/article/abs/pii/S1359431117319269

[3] Balli, O., "Exergy modeling for evaluating sustainability level of a high by-pass turbofan engine used on Commercial Aircrafts," Applied Thermal Engineering Volume 123, August 2017, Pages 138-155, *Applied Thermal Engineering* Available: https://www.sciencedirect.com/science/article/abs/pii/S1359431117319269

[4] Balli, O., "Exergy modeling for evaluating sustainability level of a high by-pass turbofan engine used on Commercial Aircrafts," Applied Thermal Engineering Volume 123, August 2017, Pages 138-155, *Applied Thermal Engineering* Available: https://www.sciencedirect.com/science/article/abs/pii/S1359431117319269

[5] Aygun, H., Cilgin, M. E., Ekmekci, I., and Turan, O., "Energy and performance optimization of an adaptive cycle engine for next generation combat aircraft," Energy Volume 209, 15 October 2020, 118261, *Energy* Available: https://www.sciencedirect.com/science/article/abs/pii/S0360544220313682.

[6] Aygun, H., Sheikhi, M. R., and Kirmizi, M., "Parametric study on Exergy and NOx metrics of turbofan engine under different design variables," Parametric Study on Exergy and NOx Metrics of Turbofan Engine Under Different Design Variables J. Energy Resour. Technol. Jun 2022, 144(6): 062303 (8 pages), *ASME Digital Collection* Available: https://asmedigitalcollection.asme.org/energyresources/article-abstract/144/6/062303/1115555/Parametric-Study-on-Exergy-and-NOx-Metrics-of?redirectedFrom=fulltext.

[7] Turan, O., "An exergy way to quantify sustainability metrics for a high bypass turbofan engine," Energy Volume 86, 15 June 2015, Pages 722-736, *Energy* Available: https://www.sciencedirect.com/science/article/abs/pii/S0360544215004582.

[8] Turan, O., "An exergy way to quantify sustainability metrics for a high bypass turbofan engine," Energy Volume 86, 15 June 2015, Pages 722-736, *Energy* Available: https://www.sciencedirect.com/science/article/abs/pii/S0360544215004582.

[9] Balli, O., and Caliskan, H., "Turbofan engine performances from aviation, thermodynamic and environmental perspectives," Energy Volume 232, 1 October 2021, 121031, *Energy* Available: https://www.sciencedirect.com/science/article/abs/pii/S0360544221012792.

[10] Balli, O., and Caliskan, H., "Turbofan engine performances from aviation, thermodynamic and environmental perspectives," Energy Volume 232, 1 October 2021, 121031, *Energy* Available: https://www.sciencedirect.com/science/article/abs/pii/S0360544221012792.

[11] Akdeniz, H. Y., and Balli, O., "Impact of different fuel usages on thermodynamic performances of a high bypass turbofan engine used in Commercial Aircraft," Energy Volume 238, Part A, 1 January 2022, 121745, *Energy* Available: https://www.sciencedirect.com/science/article/abs/pii/S0360544221019939.

[12] *Asmedigitalcollection.asme.org,* Turbo Expo: Power for Land, Sea, and Air Paper No: 78-GT-198, V01BT02A096; 13 pages https://doi.org/10.1115/78-GT-198, Published Online: April 17, 2015, Available: https://asmedigitalcollection.asme.org/GT/proceedings/GT1978/79726/V01BT02A096/230 936.

[13] Szczepankowski, A., and Przysowa, R., "Thermal degradation of turbine components in a military turbofan", Engineering Failure Analysis Volume 134, April 2022, 106088 *Engineering Failure Analysis* Available: https://www.sciencedirect.com/science/article/pii/S1350630722000620.

[14] Szczepankowski, A., and Przysowa, R., "Thermal degradation of turbine components in a military turbofan", Engineering Failure Analysis Volume 134, April 2022, 106088 *Engineering Failure Analysis* Available: https://www.sciencedirect.com/science/article/pii/S1350630722000620

[15] "Afterburner," *SKYbrary Aviation Safety* Available: https://skybrary.aero/articles/afterburner.

[16] "Aircraft Propulsion" Farokhi, Saeed. Aircraft Propulsion: Cleaner, Leaner, and Greener. United Kingdom, Wiley, 2021. *Google Books* Available: https://www.google.com/books/edition/Aircraft_Propulsion/8QY7EAAAQBAJ?hl=en&gb pv=1&dq=augmented%2Bturbofan&pg=PA156&printsec=frontcover.

[17] "Combustion in advanced gas turbine systems", Combustion in Advanced Gas Turbine Systems: Proceedings of an International Propulsion Symposium Held at the College of Aeronautics, Cranfield, April 1967. United Kingdom, Elsevier Science, 2014. *Google Books* Available: https://www.google.com/books/edition/Combustion_in_Advanced_Gas_Turbine_Syste/_p KjBQAAQBAJ?hl=en&gbpv=1&dq=augmented%2Bturbofan&pg=PA129&printsec=front cover.

[18] Mattingly, J. D., and Ohain, V. H., *Elements of gas turbine propulsion*, New Delhi: McGraw-Hill Education, 2014.

[19] "General Electric GE90," *Academic Dictionaries and Encyclopedias* Available: https://en-academic.com/dic.nsf/enwiki/244277.

[20] *Ancile* Available: https://www.deagel.com/Propulsion%20Systems/GE90/a001376.

[21] "Turbofan engines", Transport Phenomena in Multiphase Systems 2006, Pages 1-106 *Turbofan Engines - an overview | ScienceDirect Topics* Available: https://www.sciencedirect.com/topics/engineering/turbofan-engines.

[22] Mattingly, J. D., and Ohain, V. H., *Elements of gas turbine propulsion*, New Delhi: McGraw-Hill Education, 2014.

[23] Mattingly, J. D., and Ohain, V. H., *Elements of gas turbine propulsion*, New Delhi: McGraw-Hill Education, 2014.

[24] Mattingly, J. D., and Ohain, V. H., *Elements of gas turbine propulsion*, New Delhi: McGraw-Hill Education, 2014.

[25] "GE Announces Record Year for the world's largest, most powerful jet engine," *GE News* Available: https://www.ge.com/news/press-releases/ge-announces-record-year-worlds-largest-most-powerful-jet-engine.

[26] "Turbofan engines," *Turbofan Engines - an overview | ScienceDirect Topics* Available: https://www.sciencedirect.com/topics/engineering/turbofan-engines.

[27] Mattingly, J. D., and Ohain, V. H., *Elements of gas turbine propulsion*, New Delhi: McGraw-Hill Education, 2014.

[28] Mattingly, J. D., and Ohain, V. H., *Elements of gas turbine propulsion*, New Delhi: McGraw-Hill Education, 2014.

[29] Mattingly, J. D., and Ohain, V. H., *Elements of gas turbine propulsion*, New Delhi: McGraw-Hill Education, 2014.

[30] Mattingly, J. D., and Ohain, V. H., *Elements of gas turbine propulsion*, New Delhi: McGraw-Hill Education, 2014.

[31] Mattingly, J. D., and Ohain, V. H., *Elements of gas turbine propulsion*, New Delhi: McGraw-Hill Education, 2014.

[32] Mattingly, J. D., and Ohain, V. H., *Elements of gas turbine propulsion*, New Delhi: McGraw-Hill Education, 2014.

Appendix

MATLAB code used for the parametric cycle analysis of the turbofan engine:

```matlab
clear all;
close all;
clc;
Alt = 12000;
Temp = 355;
Press = 25000;
Mach_Nums = 0:1.0:5.0;
Sht = 1250;
Spt = 1050;
gamma_c = 1.4;
gamma_h = 1.35;
h_PR = 20000*10^3;
Diff = 0.50;
Press_Ratio_Fan = 3.0;
Press_Compress = 7.50;
Press_HCompress = 1.50;
Assum_a = 0.7;
Assum_b = 0.7;
Assum_c = 0.72;
Assum_d = 0.72;
Assum_e = 0.72;
Assum_f = 0.79;
ass_G = 0.74;
nu_b = 0.79;
MFR = 400;
Fuel_MFR = 2.500;
Tt6 = 1500:6:2500;
Assum_I = 0.79;
Lam_1 = 0.50;
Lam_2 = 1;
Lam_3 = 1;
Press_burn = 0.05;
Press_FanDuct = 0;
A = Fuel_MFR/MFR;
Beta = 5.6;
AB = ((gamma_c-1)/gamma_c)*Spt;
CD = ((gamma_h-1)/gamma_h)*Sht;
c = sqrt(gamma_c*AB*Temp);
Velo = c.*Mach_Nums;
figure,
plot(Mach_Nums, Velo, 'b');
xlabel('Mach Number');
ylabel('Velocity [m/s]');
title('Velocity vs. Mach Number');
set(findall(gcf,'type','line'), 'linewidth',3);
set(gca, 'fontsize', 10);
grid on
TempRat = 1+(((gamma_c-1)/2)*Mach_Nums.^2);
PressRat = TempRat.^(gamma_c/(gamma_c-1));
```

```matlab
Tt2 = Temp.*TempRat;
Pt2 = Diff.*Press.*PressRat;
figure,
plot(Mach_Nums, Tt2, 'b');
xlabel('Mach Number');
ylabel('Temperature at Inlet [K]');
title('Temperature at Inlet vs. Mach Number');
set(findall(gcf,'type','line'), 'linewidth',3);
set(gca, 'fontsize', 10);
grid on
figure,
plot(Mach_Nums, Pt2, 'b');
xlabel('Mach Number');
ylabel('Pressure at Inlet [Pa]');
title('Pressure at Inlet vs. Mach Number');
set(findall(gcf,'type','line'), 'linewidth',3);
set(gca, 'fontsize', 10);
grid on
Pt3 = Pt2.*Press_Ratio_Fan;
Tt3 = Tt2.*(1+((Press_Ratio_Fan^(gamma_c-1/gamma_c)-1)/ass_G));
figure,
plot(Mach_Nums, Tt3, 'b');
xlabel('Mach Number');
ylabel('Temperature of the Fan [K]');
title('Temperature of the Fan vs. Mach Number');
set(findall(gcf,'type','line'), 'linewidth',3);
set(gca, 'fontsize', 10);
grid on
figure,
plot(Mach_Nums, Pt3, 'b');
xlabel('Mach Number');
ylabel('Pressure of the Fan [Pa]');
title('Pressure of the Fan vs. Mach Number');
set(findall(gcf,'type','line'), 'linewidth',3);
set(gca, 'fontsize', 10);
grid on
Pt4 = Pt3.*Press_Compress;
Tt4 = Tt3.*(1 + Press_Compress^((gamma_c-1)/gamma_c)-1)/Assum_a;
figure,
plot(Mach_Nums, Tt4, 'b');
xlabel('Mach Number');
ylabel('Temperature of the Compressor [K]');
title('Temperature of the Compressor vs. Mach Number');
set(findall(gcf,'type','line'), 'linewidth',3);
set(gca, 'fontsize', 10);
grid on
figure,
plot(Mach_Nums, Pt4, 'b');
xlabel('Mach Number');
ylabel('Pressure of the Compressor [Pa]');
title('Pressure of the Compressor vs. Mach Number');
set(findall(gcf,'type','line'), 'linewidth',3);
set(gca, 'fontsize', 10);
grid on
Pt5 = Pt4.*Press_HCompress;
```

```matlab
Tt5 = Tt4.*(1+(Press_HCompress^((gamma_c-1)/gamma_c)-1)/Assum_b);
figure,
plot(Mach_Nums, Tt5, 'b');
xlabel('Mach Number');
ylabel('Temperature of the High Compressor [K]');
title('Temperature of the High Compressor vs. Mach Number');
set(findall(gcf,'type','line'), 'linewidth',3);
set(gca, 'fontsize', 9);
grid on
figure,
plot(Mach_Nums, Pt5, 'b');
xlabel('Mach Number');
ylabel('Pressure of the High Compressor [Pa]');
title('Pressure of the High Compressor vs. Mach Number');
set(findall(gcf,'type','line'), 'linewidth',3);
set(gca, 'fontsize', 10);
grid on
```